Electronic Supplementary Material (ESI) for Chemical Communications.


# Supporting Information

## A Case of Alkylidyne-Imine Metathesis

Rinku Yadav, Ion Ghiviriga, Khalil A. Abboud, Adam S. Veige*

Department of Chemistry, University of Florida, Center for Catalysis, P.O. Box 117200, Gainesville, Florida 32611, United States.

# Contents

## EXPERIMENTAL SECTION

## 1. General Considerations

Unless otherwise specified, all manipulations were performed under an inert atmosphere using standard Schlenk or glove-box techniques. Glassware was oven-dried before use. Pentane, hexane, toluene, diethyl ether ($Et_2O$), tetrahydrofuran (THF), benzene ($C_6H_6$) were dried using a GlassContour drying column and stored over 3 Å molecular sieves. Benzene-$d_6$ (Cambridge Isotopes) was dried over sodium benzophenone distilled, and stored over 3 Å molecular sieves. The tungsten-alkylidyne [$^t$BuOCO]W≡C$^t$Bu(THF)$_2$ (**1**)[1] was prepared according to published procedures. *N*-methyl-1-phenylmethanimine and *N*-benzyl-1-phenylmethanimine were bought from sigma –Aldrich, *N*,1-diphenylmethanimine and *N*-(trimethylsilyl)-1-phenylmethanimine were bought from Oakwood chemicals, and other imines were synthesized according to reported literature.[2–4] Liquid imines were dried over $CaH_2$ and stored under a nitrogen atmosphere, solid imines were dried under vacuum overnight before use. $^1$H NMR, $^{13}$C{$^1$H} NMR and 2D NMR spectra were obtained on Varian INOVA (500 MHz) and Bruker (400 MHz) spectrometers. The chemical shifts are reported in δ (ppm), referenced to the lock signal on solvent for $^1$H and $^{13}$C{$^1$H} spectra. The assignments are primarily based on the cross-peaks observed in the $^1$H-$^{13}$C gradient Hetronuclear Multiple Bond Correlation (gHMBC), gradient Hetronuclear Single Quantum Correlation (gHSQC), $^1$H-$^1$H Homonuclear Correlation Spectroscopy (COSY) and Nuclear Overhauser Effect Spectroscopy (NOESY) spectra. The spectra were recorded at 25 °C unless noted otherwise. Elemental analyses were performed at the CENTC Elemental Analysis Facility, Department of Chemistry at University of Rochester.

## 2. Synthetic procedures

### 2.1. Synthesis of complex 2

Complex **1** (101 mg, 13.1 x $10^{-2}$ mmol, 1.00 eq) was dissolved in 5 mL of benzene in a vial equipped with a magnetic stir bar and 3,4-dihydroisoquinoline (17.0 mg, 13.1 x $10^{-2}$ mmol, 1.00 eq) was added to the solution at room temperature and stirred for 1 h. The color of the solution immediately changed from red to dark brown. Volatiles were removed under vacuum yielding **2** as a dark red solid, it was further washed with 5 mL of cold pentane to yield **2** (93.8 mg, 95% yield). Maroon colored crystals of **2** can be obtained from a concentrated solution of **2** in either pentane or toluene at -30 °C within a 2 d.

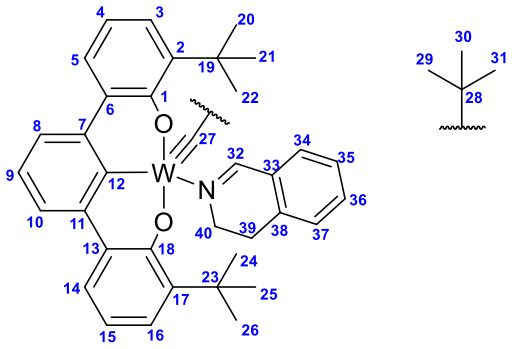

$^{1}$H NMR ($C_6D_6$, 400 MHz) δ (ppm): 8.49 (s, 1H, $H_{32}$), 8.10 (d, 2H, $J$ = 7.8 Hz, Ar-$H_{8,10}$), 7.93 (dd, 2H, $J_1$ = 7.9 Hz, $J_2$ = 1.6 Hz, Ar-$H_{5,14}$), 7.44 (m, 3H, Ar-$H_{3,9,16}$), 7.08 (t, 2H, $J$ = 1.6 Hz, Ar-$H_{4,15}$), 6.98 (m, 1H, Ar-$H_{37}$), 6.84 (m, 2H, Ar-$H_{36,35}$), 6.65 (d, 1H, $J$ = 7.4 Hz, Ar-$H_{34}$), 3.69 (t, 2H, J = 7.7 Hz, Ar-$H_{40}$), 2.44 (t, 2H, $J$ = 7.7 Hz, Ar-$H_{39}$), 1.57 (s, 18H, Ar-$^t$Bu, $H_{20\text{-}22,24\text{-}26}$), 0.70 (s, 9H, W≡C$^t$Bu, $H_{29\text{-}31}$).

$^{13}$C{$^{1}$H}NMR ($C_6D_6$, 400 MHz) δ (ppm): 320.8 ($C_{27}$), 193.1 ($C_{12}$), 171.8 ($C_{32}$), 163.2 ($C_{1,18}$), 140.2 ($C_{7,11}$), 136.5 ($C_{38}$), 135.2 ($C_{6,13}$), 135.0 ($C_{37}$), 134.7 ($C_{2,17}$), 130.7 ($C_{36}$), 127.9 ($C_{5,14}$), 127.8 ($C_{34}$), 127.3 ($C_{35}$), 127.0 ($C_{8,10}$), 126.6 ($C_{33}$), 124.7 ($C_{3,16,9}$), 120.8 ($C_{4,15}$), 50.0 ($C_{28}$), 49.3 ($C_{40}$), 35.2 ($C_{19,23}$), 32.7 ($C_{29\text{-}31}$), 30.4 ($C_{20\text{-}22,24\text{-}26}$), 25.1 ($C_{39}$).

### 2.2. Synthesis of complex 3

Complex **1** (100 mg, 13.0 x $10^{-2}$ mmol, 1.00 eq) was dissolved in 5 mL of benzene in a vial equipped with a magnetic stir bar and 3,4-dihydroisoquinoline (85.2 mg, 65.2 x $10^{-2}$ mmol, 5.00 eq) was added to the solution at room temperature and stirred for 1 h. NMR spectral data of the reaction mixture reveals that complexes **2** and **3** coexist in the solution in ratio 1:2.5, respectively under these conditions. Volatiles were removed under vacuum. A brown precipitate (120.4 mg) was obtained after 3-4 triturations using pentane. Separation of **3** via crystallization was not possible. In situ solution NMR characterization of **3** is provided below.

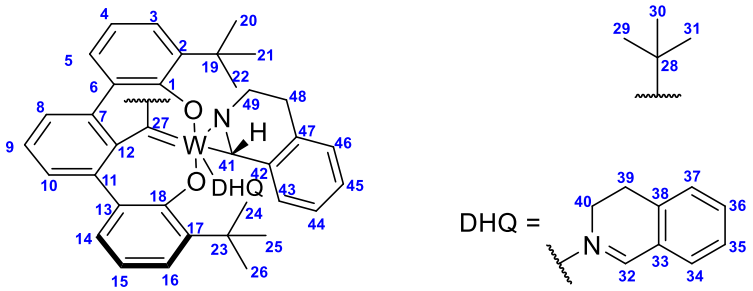


$^{1}$H NMR ($C_6D_6$, 500 MHz) δ (ppm): 8.50 (t, 1H, $J$ = 1.6 Hz, $H_{32}$), 7.40 (dd, 1H, $J_1$ = 6.3 Hz, $J_2$ = 1.2 Hz, Ar-$H_{10}$), 7.38 (dd, 1H, $J_1$ = 6.5 Hz, $J_2$ = 1.5 Hz Ar-$H_{16}$), 7.33 (m, 1H, $J_1$ = 6.2 Hz, $J_2$ = 1.3 Hz, Ar-$H_{14}$), 7.30 (dd, 1H, $J_1$ = 6.4 Hz, $J_2$ = 1.5 Hz, Ar-$H_3$), 7.28 (dd, 1H, $J_1$ = 6.3 Hz, $J_2$ = 1.4 Hz, Ar-$H_8$), 7.26 (dd,

1H, $J_1$ = 6.2 Hz, $J_2$ = 1.5 Hz, Ar-$H_5$), 7.21 (m, 1H, Ar-$H_{43}$), 7.16 (m, 1H, Ar-$H_{44}$), 7.09 (t, 1H, $J$ = 6.3 Hz, Ar-$H_9$), 7.06 (m, 1H, Ar-$H_{46}$), 7.00 (m, 1H, $H_{45}$), 6.91 (m, 1H, Ar-$H_{36}$), 6.86 (t, 1H, $J$ = 6.3 Hz, Ar-$H_{15}$), 6.81 (t, 1H $J$ = 6.1 Hz, Ar-$H_4$), 6.77 (m, 1H, Ar-$H_{35}$), 6.71 (m, 1H, Ar-$H_{34}$), 6.54 (d, 1H, $J$ = 6.1 Hz, Ar-$H_{37}$), 5.15 (ddd, 1H, $J_1$ = 10.4 Hz, $J_2$ = 8.1 Hz, $J_3$ = 4.9 Hz, Ar-$H_{49'}$), 5.06 (ddd, 1H, $J_1$ = 10.4 Hz, $J_2$ = 6.1 Hz, $J_3$ = 2.6 Hz, Ar-$H_{49''}$), 3.91 (s, 1H, $H_{41}$), 3.66 (td, 2H, $J_1$ = 6.4 Hz, $J_2$ = 1.6 Hz, Ar-$H_{40}$), 3.13 (m, 1H, Ar-$H_{48a}$), 2.90 (ddd, 1H, , $J_1$ = 13.4 Hz, $J_2$ = 5.1 Hz, $J_3$ = 2.6 Hz, Ar-$H_{48b}$), 2.10 (m, 2H, $H_{39}$), 1.50 (s, 9H, Ar-$^t$Bu, $H_{24\text{-}26}$), 1.04 (s, 9H, Ar-$^t$Bu, $H_{20\text{-}22}$), 0.97 (s, 9H, $H_{29\text{-}31}$).

$^{13}C\{^1H\}$NMR ($C_6D_6$, 500 MHz) δ (ppm): 256.3 ($C_{27}$), 169.7 (s, $C_{18}$), 169.6 (s, $C_1$), 167.5 (s, $C_{32}$), 161.4 (s, $C_7$), 159.5 (s, $C_{11}$), 143.7 (s, $C_{42}$), 139.3 (s, $C_2$), 139.1 (s, $C_{17}$), 136.9 (s, $C_{38}$), 135.9 (s, $C_{47}$), 135.1 (s, $C_9$), 131.5 (s, $C_{13}$), 131.5 (s, $C_6$), 131..0 (s, $C_8$), 130.0 (s, $C_{10}$), 129.6 (s, $C_{34}$), 129.5 (s, $C_{46}$), 129.0 (s, $C_5$), 128.7 (s, $C_{43}$), 128.4 (s, $C_{33}$), 128.3 (s, $C_{14}$), 127.4 (s, $C_{35}$) 127.2 (s, $C_{37}$), 127.1 (s, $C_{36}$), 126.7 (s, $C_{16}$), 126.8 (s, $C_3$), 125.9 (s, $C_{44}$), 124.3 (s, $C_{45}$), 118.6 (s, $C_4$) 118.4 (s, $C_{15}$), 118.1 (s, $C_{12}$), 57.1 (s, $C_{49}$), 48.8 (s, $C_{40}$), 45.0 (s, $C_{28}$) 44.7 (s, $C_{41}$), 35.1 (s, $C_{29\text{-}31}$), 35.0 (s, $C_{23}$), 34.7 (s, $C_{19}$), 31.0 (s, $C_{48}$) 30.6 (s, $C_{20\text{-}22}$), 30.3 (s, $C_{24\text{-}26}$), 25.9 (s, $C_{39}$).

### 2.3. Synthesis of complex 4-R (R = Me, TMS, Ph, Bn)

Complex **1** (100 mg, 13.0 x $10^{-2}$ mmol, 1.00 eq) was dissolved in 5 mL of benzene in a vial equipped with a magnetic stir bar. Imine (13.0 x $10^{-2}$ mmol, 1.00 eq) was added to the above solution at room temperature resulting in a dark red solution. The resultant solution was then transferred to a Schlenk tube equipped with a magnetic stir bar and heated at 80 °C in an oil bath for 2 d for *N*-methyl-1-phenylmethanimine (color changed to transparent yellow) and *N*-benzyl-1-phenylmethanimine (color changed to transparent amber), and 4d for *N*,1-diphenylmethanimine (color changed to transparent yellow) and *N*-(trimethylsilyl)-1-phenylmethanimine (color changed to transparent yellow). Volatiles were removed under vacuum precipitating **4-R** in 95-98% yields. **4-Me** and **4-Bn** were crystallized from concentrated pentane solutions as yellow crystals at -30 °C. **4-Ph** and **4-TMS** were crystallized from concentrated $Et_2O$:THF (9:1) solutions as yellow crystals at -30 °C.

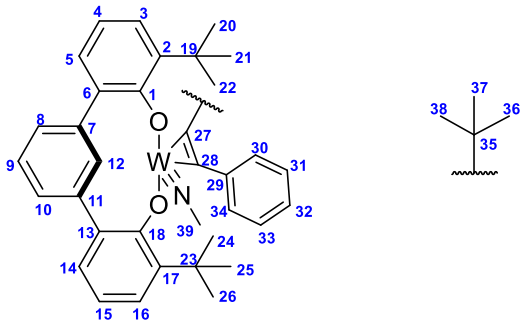

**4-Me**, $^{1}$H NMR ($C_6D_6$, 500 MHz) δ (ppm): 7.99 (t, 1H, $J$ = 1.9 Hz, Ar-$H_{12}$), 7.34 (d, 1H, $J$ = 7.4 Hz, Ar-$H_{16}$), 7.28 (d, 1H, $J$ = 7.7 Hz, Ar-$H_3$), 7.18 (d, 1H, $J$ = 1.7 Hz, Ar-$H_{14}$), 7.16 (d, 2H, $J$ = 1.6 Hz, Ar-$H_{30,34}$), 7.13 (t, 1H, $J$ = 9.6 Hz, Ar-$H_9$), 7.02 (m, 2H, Ar-$H_{31,33}$), 6.99 (m, 1H, Ar-$H_{10}$), 6.93 (m, 2H, Ar-$H_{5,15}$), 6.85 (tt, 1H, $J_1$ = 9.2 Hz, $J_2$ = 1.7 Hz, Ar-$H_{37}$), 6.75 (t, 1H, $J$ = 9.7 Hz, Ar-$H_4$), 6.64 (d, 1H, $J$ = 9.5 Hz, Ar-$H_8$), 4.00 (s, 3H, $H_{39}$), 1.69 (s, 9H, Ar-$^t$Bu, $H_{24-26}$), 1.68 (s, 9H, Ar-$^t$Bu, $H_{20-22}$), 1.10 (s, 9H, $H_{36-38}$).

$^{13}$C{$^{1}$H}NMR ($C_6D_6$, 500 MHz) δ (ppm): 198.3 ($C_{27}$), 180.3 ($C_{28}$), 162.0 ($C_{18}$), 161.4 ($C_1$), 142.6 ($C_{11}$), 141.7 ($C_7$), 141.1 ($C_{17}$), 138.6 ($C_{29}$), 133.6 ($C_{13}$), 132.5 ($C_6$), 130.9 ($C_{10,30,34}$), 129.7 ($C_8$), 127.6 ($C_{12}$), 127.3 ($C_{31,33}$), 127.1 ($C_{32}$), 127.0 ($C_{14}$), 126.9 ($C_5$), 126.9 ($C_{16}$), 126.9 ($C_3$), 122.9 ($C_{15}$), 122.4 ($C_4$), 51.6 ($C_{39}$), 42.3 (s, $C_{35}$), 35.7 (s, $C_{19,23}$), 31.9 (s, $C_{36-38}$), 30.2 (s, $C_{20-22,24-26}$).

Elemental Analysis calcd. (%) for $C_{39}H_{45}NO_2W$ (743.63 g/mol): C, 62.990; H, 6.100; N, 1.884; Found: C, 62.605; H, 5.904; N, 1.795.

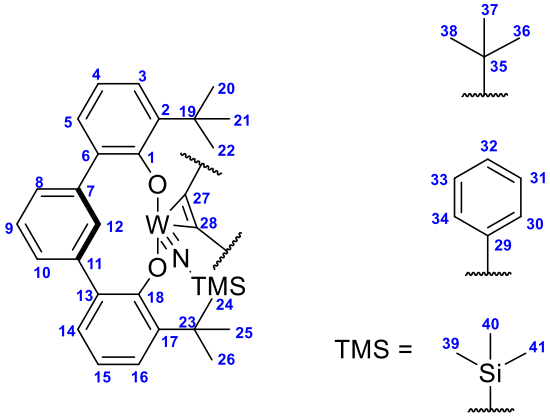


**4-TMS**, $^{1}$H NMR ($C_6D_6$, 400 MHz) δ (ppm): 7.90 (t, 1H, $J$ = 7.6 Hz, Ar-$H_{12}$), 7.33 (dd, 1H, $J_1$ = 1.8 Hz, $J_2$ = 7.8 Hz, Ar-$H_{16}$), 7.26 (dd, 1H, $J_1$ = 1.8 Hz, $J_2$ = 7.8 Hz, Ar-$H_3$), 7.21(m, 2H, Ar-$H_{30,34}$), 7.19 (dd, 1H, $J_1$ = 1.8 Hz, $J_2$ = 7.8 Hz, Ar-$H_{14}$), 7.13(t, 1H, $J$ = 7.6 Hz, Ar-$H_9$), 7.02 (m, 2H, Ar-$H_{31,33}$), 7.00 (m, 1H, Ar-$H_{10}$), 6.93 (dd, 1H, $J_1$ = 1.8 Hz, $J_2$ = 7.8 Hz, Ar-$H_5$), 6.91 (t, 1H, $J$ = 7.8 Hz, Ar-$H_{15}$), 6.83 (tt, 1H, $J_1$ = 1.3 Hz, $J_2$ = 7.4 Hz, Ar-$H_{32}$), 6.74 (t, 1H, $J$ = 7.8 Hz, Ar-$H_4$), 6.70 (ddd, 1H, $J_1$ = 1.1 Hz, $J_2$ = 1.8 Hz, $J_3$ = 7.6 Hz, Ar-$H_8$), 1.71 (s, 9H, Ar-$^t$Bu, $H_{24-26}$), 1.69 (s, 9H, Ar-$^t$Bu, $H_{20-22}$), 1.12 (s, 9H, $H_{36-38}$), 0.25 (s, 9H, TMS, $H_{39-41}$).

$^{13}$C{$^{1}$H}NMR ($C_6D_6$, 400 MHz) δ (ppm): 196.7 ($C_{27}$), 180.0 ($C_{28}$), 161.7 ($C_{18}$), 161.0 ($C_1$), 141.5 ($C_{11}$), 140.9 ($C_{17}$), 140.8 ($C_2$), 140.7 ($C_7$), 138.4 ($C_{29}$), 133.8 ($C_{13}$), 132.8 ($C_6$), 131.1 ($C_9$), 130.9 ($C_{30,34}$), 129.3 ($C_{10}$), 129.1 ($C_{12}$), 128.1 ($C_8$), 127.4 ($C_{31,34}$), 127.3 ($C_{32}$), 127.1 ($C_{14}$), 126.9 ($C_5$), 126.8 ($C_{3,16}$), 123.2 ($C_{15}$), 122.8 ($C_4$), 41.6 ($C_{35}$), 35.8 ($C_{23}$), 35.7 ($C_{19}$), 31.7 ($C_{36-38}$), 30.5 ($C_{24-26}$), 30.4 ($C_{20-22}$), 2.71 ($C_{39-41}$).

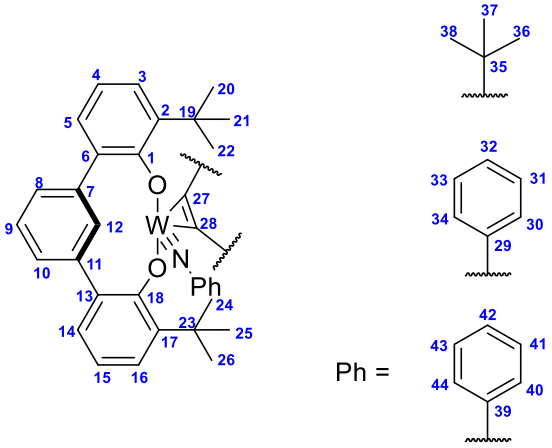


**4-Ph**, $^{1}$H NMR ($C_6D_6$, 400 MHz) δ (ppm): 8.00 (t, 1H, $J$ = 1.8 Hz, Ar-$H_{12}$), 7.34 (dd, 1H, $J_1$ = 1.7 Hz, $J_2$ = 7.8 Hz, Ar-$H_{16}$), 7.32 (dd, 2H, $J_1$ = 1.2 Hz, $J_2$ = 8.2 Hz, Ar-$H_{30,34}$), 7.27 (dd, 1H, $J_1$ = 1.7 Hz, $J_2$ = 7.8 Hz, Ar-$H_3$), 7.18 (dd, 1H, $J_1$ = 1.7 Hz, $J_2$ = 7.4 Hz, Ar-$H_{14}$), 7.14 (dd, 2H, $J_1$ = 1.3 Hz, $J_2$ = 8.6 Hz, Ar-$H_{40,44}$), 7.12 (t, 1H, $J$ = 7.7 Hz, Ar-$H_9$), 7.05 (m, 4H, Ar-$H_{31,33,41,43}$), 6.99 (ddd, 1H, $J_1$ = 1.2 Hz, $J_2$ = 1.8 Hz, $J_3$ = 7.7 Hz, Ar-$H_{10}$), 6.92 (t, 1H, $J$ = 7.8 Hz, Ar-$H_{15}$), 6.91 (dd, 1H, $J_1$ = 1.7 Hz, $J_2$ = 7.8 Hz, Ar-$H_5$), 6.87 (tt, 1H, $J_1$ = 1.3 Hz, $J_2$ = 7.4 Hz, Ar-$H_{42}$), 6.75 (t, 1H, $J$ = 7.8 Hz, Ar-$H_4$), 6.73 (tt, 1H, $J_1$ = 1.2 Hz, $J_2$ = 7.2 Hz, Ar-$H_{32}$), 6.63 (ddd, 1H, $J_1$ = 1.2 Hz, $J_2$ = 1.8 Hz, $J_3$ = 7.7 Hz, Ar-$H_8$), 1.73 (s, 9H, Ar-$^t$Bu, $H_{24-26}$), 1.64 (s, 9H, Ar-$^t$Bu, $H_{20-22}$), 1.07 (s, 9H, $H_{36-38}$).

$^{13}$C{$^{1}$H}NMR ($C_6D_6$, 400 MHz) δ (ppm): 203.3 ($C_{27}$), 183.9 ($C_{28}$), 161.8 ($C_{18}$), 161.0 ($C_1$), 157.2 ($C_{39}$), 142.7 ($C_{11}$), 141.7 ($C_7$), 141.3 ($C_{17}$), 141.2 ($C_2$), 137.9 ($C_{29}$), 133.7 ($C_{13}$), 132.5 ($C_6$), 131.7 ($C_9$), 131.3 ($C_{41,43}$), 129.8 ($C_{10}$), 128.5 ($C_8$), 127.7 ($C_{31,33}$), 127.6 ($C_{14}$), 127.5 ($C_{16}$), 127.3 ($C_{12}$), 127.1 ($C_{42}$), 126.8 ($C_3$), 126.7 ($C_5$), 125.4 ($C_{40,44}$), 124.8 ($C_{32}$), 123.3 ($C_{15}$), 122.8 ($C_4$), 42.8 ($C_{35}$), 35.8 ($C_{23}$), 35.7 ($C_{19}$), 31.9 ($C_{36-38}$), 30.3 ($C_{24-26}$), 30.2 ($C_{20-22}$).

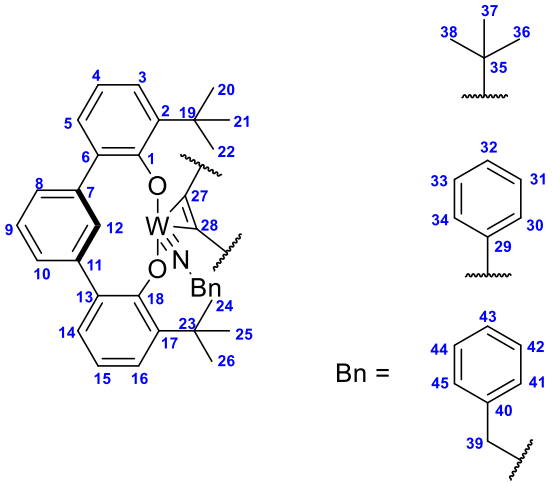

**4-Bn**, $^{1}$H NMR ($C_6D_6$, 400 MHz) δ (ppm): 8.01 (t, 1H, *J* = 1.8 Hz, Ar-$H_{12}$), 7.32 (dd, 1H, $J_1$ = 1.7 Hz, $J_2$ = 7.9 Hz, Ar-$H_{16}$), 7.28 (m, 3H, Ar-$H_{3,41,45}$), 7.17 (m, 4H, Ar-$H_{9,14,30,34}$), 7.12 (m, 2H, Ar-$H_{42,44}$), 7.02 (m, 3H, Ar-$H_{31,33,43}$), 6.98 (ddd, 1H, $J_1$ = 1.2 Hz, $J_2$ = 1.8 Hz, $J_3$ = 8.2 Hz, Ar-$H_{10}$), 6.94 (dd, 1H, $J_1$ = 1.7 Hz, $J_2$ = 7.9 Hz, Ar-$H_5$), 6.91 (t, 1H, *J* = 7.9 Hz, Ar-$H_{15}$), 6.86 (tt, 1H, $J_1$ = 1.2 Hz, $J_2$ = 7.5 Hz, Ar-$H_{32}$), 6.76 (t, 1H, J = 7.9 Hz, Ar-$H_4$), 6.64 (ddd, 1H, $J_1$ = 1.2 Hz, $J_2$ = 1.8 Hz, $J_3$ = 8.2 Hz, Ar-$H_8$), 5.39 (s, 2H, $H_{39}$), 1.62 (s, 18H, Ar-$^{t}$Bu, $H_{20\text{-}22,24\text{-}26}$), 1.04 (s, 9H, $H_{36\text{-}38}$).

$^{13}$C{$^{1}$H}NMR ($C_6D_6$, 400 MHz) δ (ppm): 198.9 ($C_{27}$), 180.9 ($C_{28}$), 161.9 ($C_{18}$), 161.3 ($C_1$), 142.4 ($C_{11}$), 141.5 ($C_7$), 141.2 ($C_{17}$), 141.1 ($C_2$), 140.1 ($C_{40}$), 138.4 ($C_{29}$), 133.7 ($C_{13}$), 132.7 ($C_6$), 131.5 ($C_9$), 131.1 ($C_{30,34,43}$), 129.6 ($C_{10}$), 128.6 ($C_{12,42,44}$), 128.2 ($C_{41,45}$), 128.0 ($C_8$) 127.3 ($C_{14,16}$), 127.2 ($C_3$), 126.9 ($C_5$), 126.8 ($C_{31,32,33}$), 122.9 ($C_{15}$), 122.5 ($C_4$), 68.3 ($C_{39}$), 42.2 ($C_{35}$), 35.7 ($C_{19,23}$), 31.8 ($C_{36\text{-}38}$), 30.1 ($C_{20\text{-}22,24\text{-}26}$).

## 3. Experimental NMR data

### 3.1. NMR spectra of 2

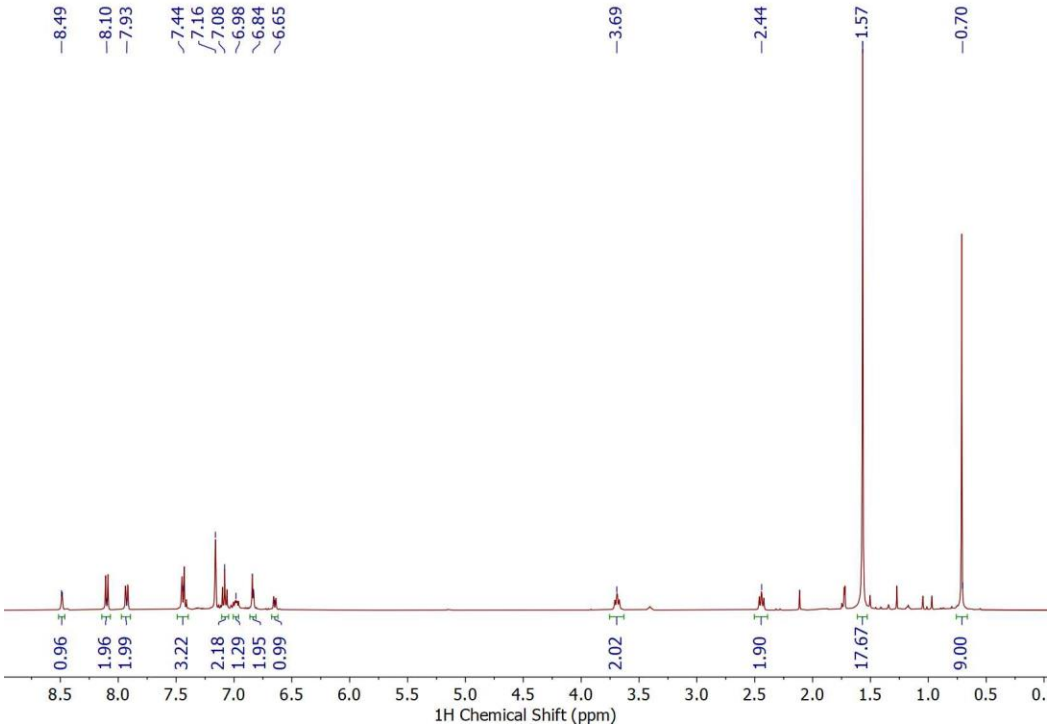


**Figure S1**. $^{1}$H NMR spectrum of **2** ($C_6D_6$, 400 MHz, 25 °C).

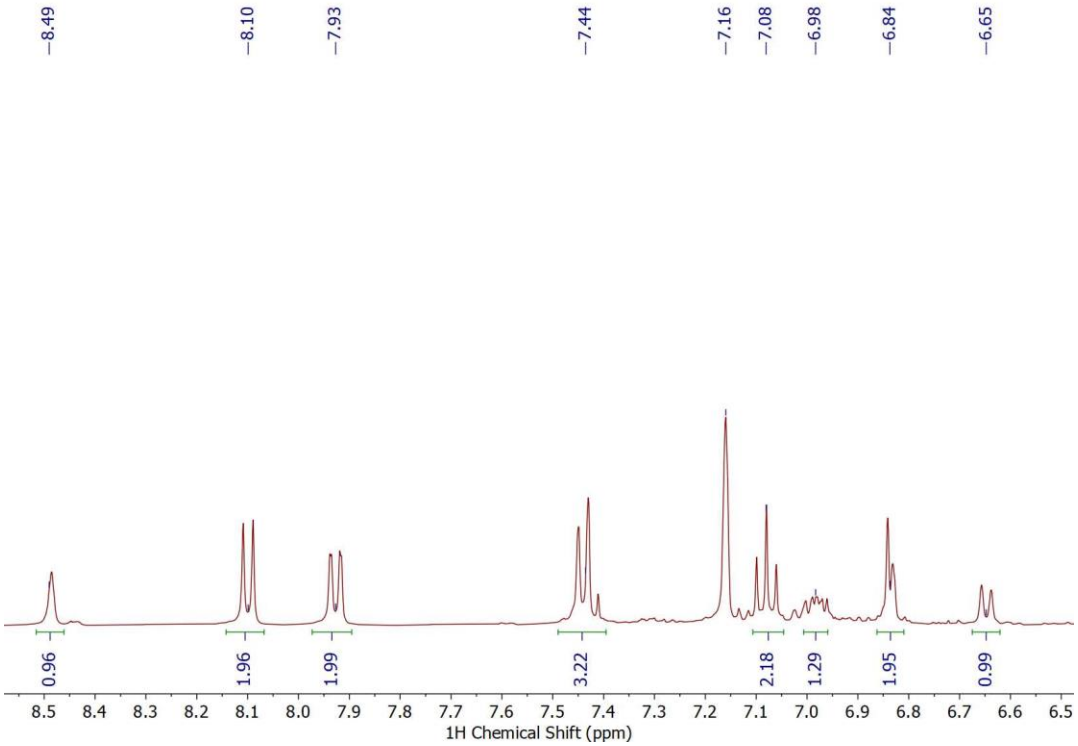


**Figure S2**. $^{1}$H NMR spectrum-expansion of **2** ($C_6D_6$, 400 MHz, 25 °C).

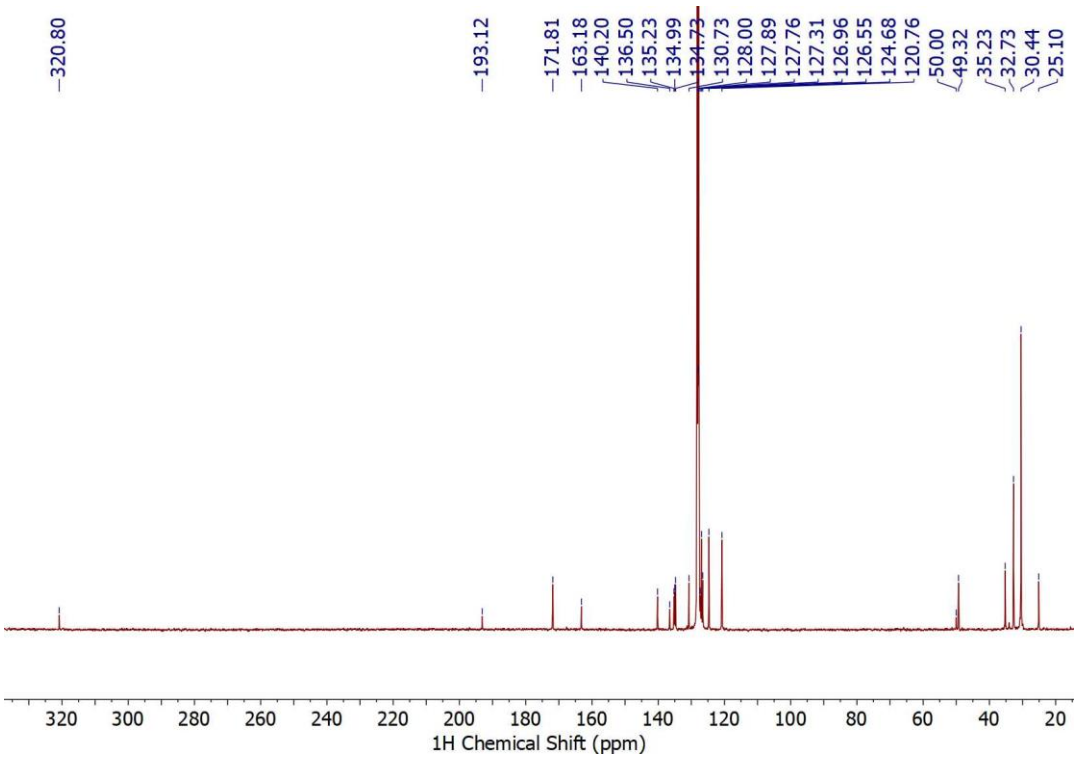


**Figure S3**. $^{13}C$ NMR spectrum of **2** ($C_6D_6$, 400 MHz, 25 °C).

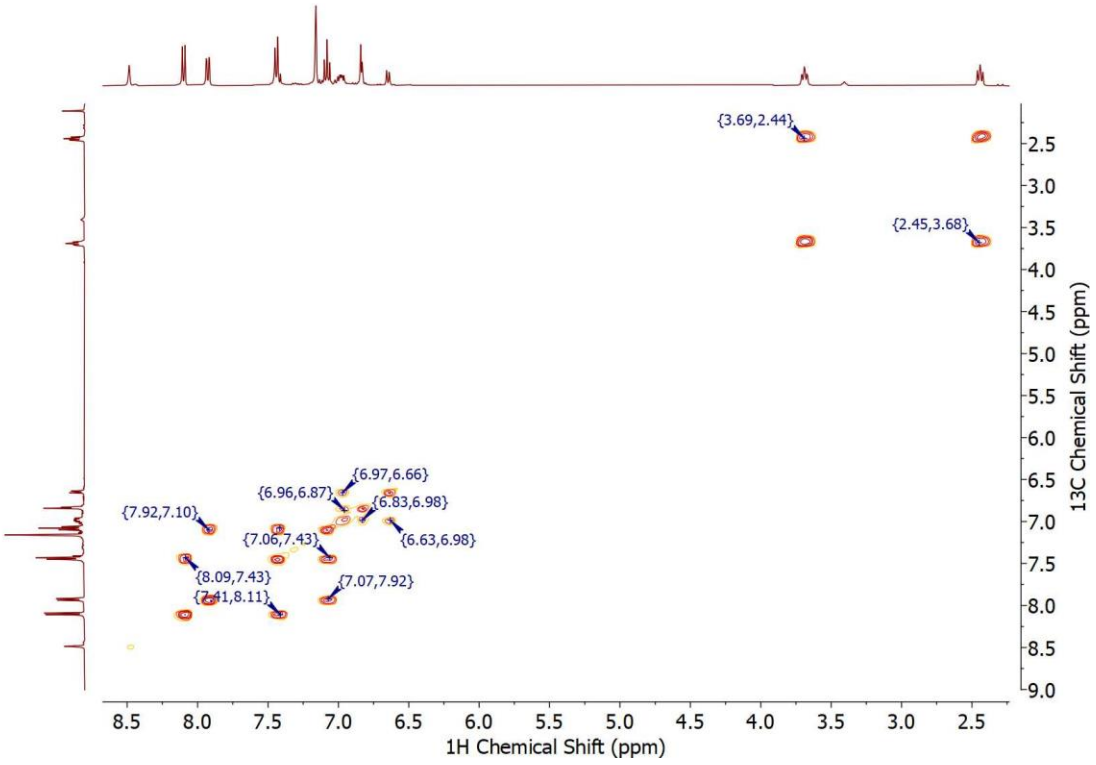


**Figure S4**. $^{1}H$-$^{1}H$ COSY NMR spectrum-expansion of **2** ($C_6D_6$, 400 MHz, 25 °C).

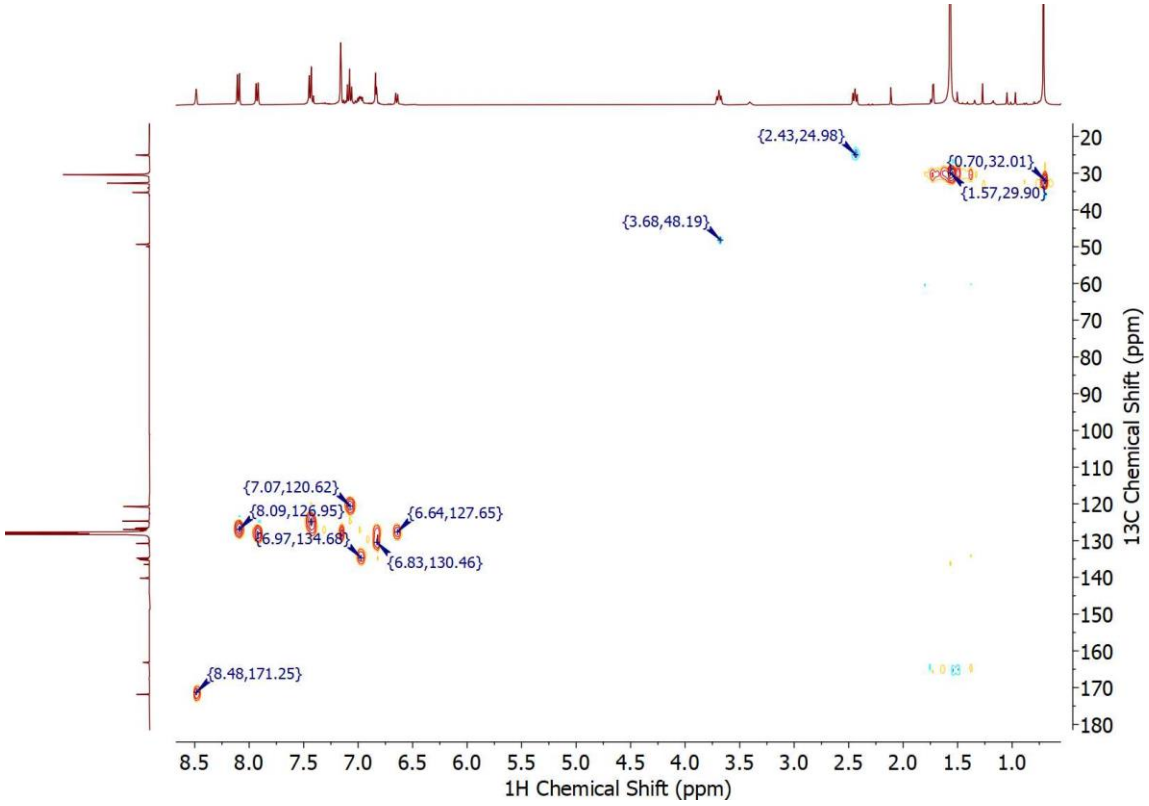


**Figure S5**. $^{1}H$-$^{13}C$ HSQC NMR spectrum of **2** ($C_6D_6$, 400 MHz, 25 °C).

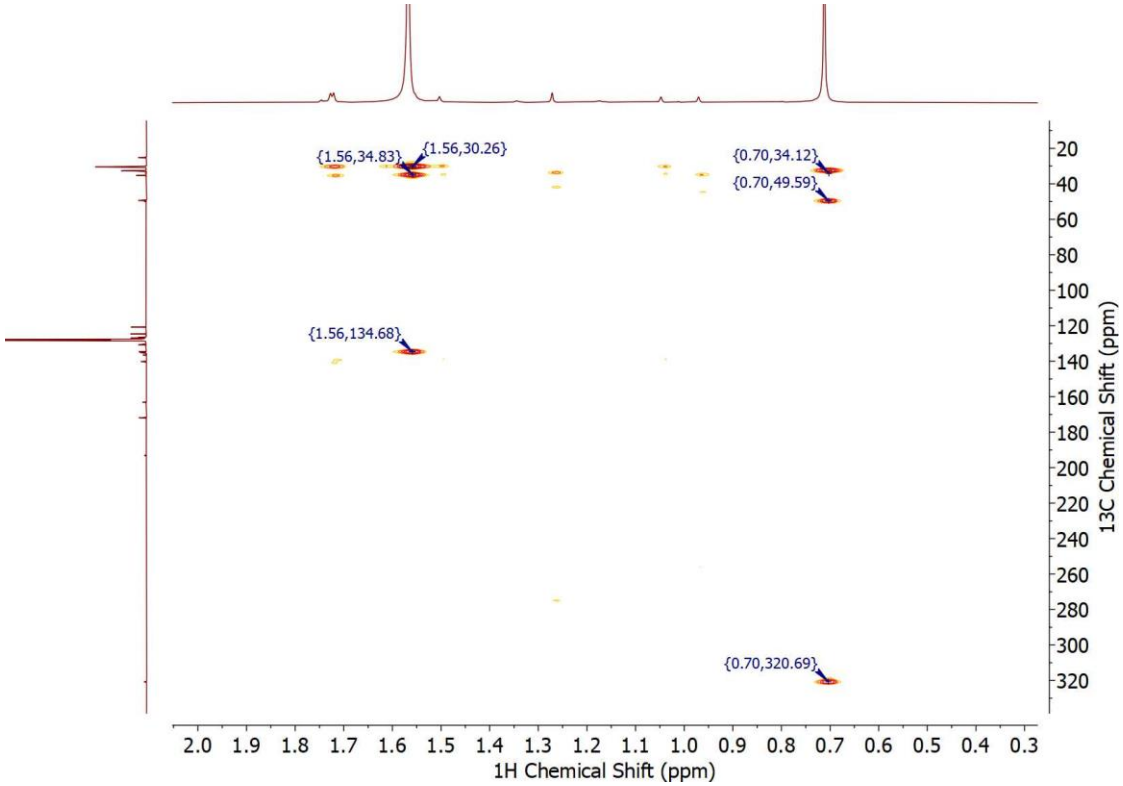


**Figure S6**. $^{1}H$-$^{13}C$ HMBC NMR spectrum-expansion of **2** ($C_6D_6$, 400 MHz, 25 °C).

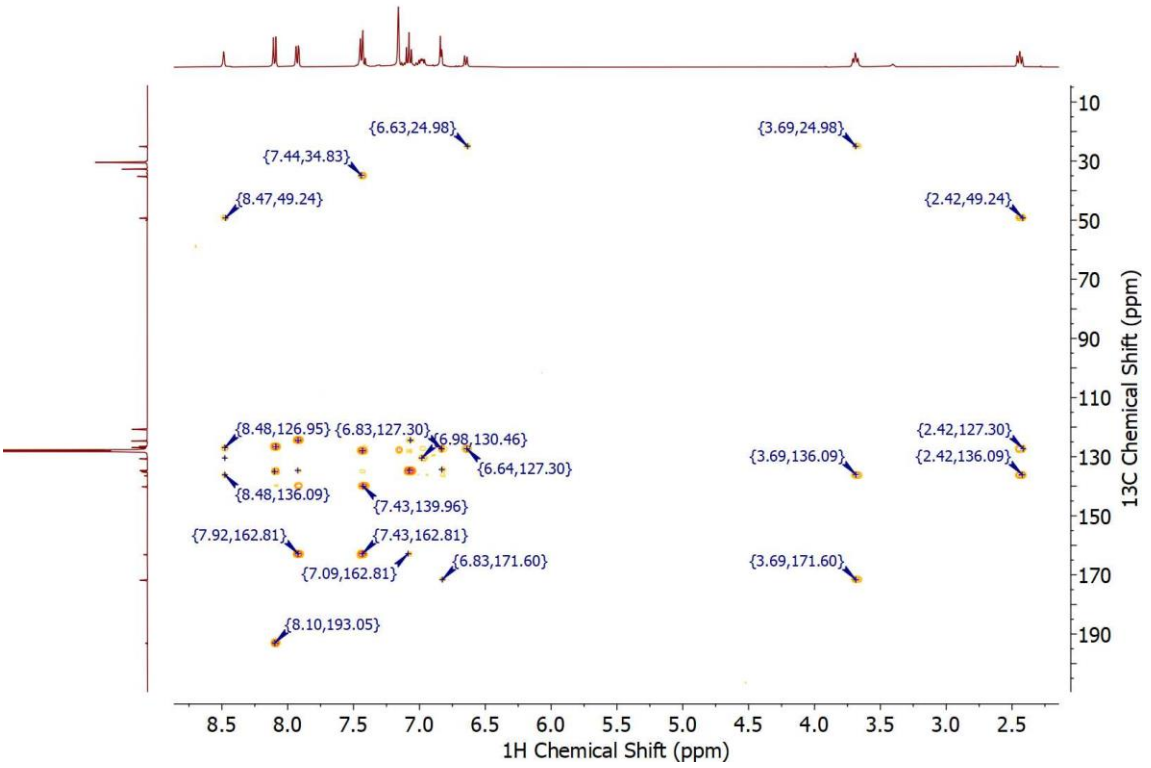


**Figure S7**. $^{1}H$-$^{13}C$ HMBC NMR spectrum-expansion of **2** ($C_6D_6$, 400 MHz, 25 °C).

## 3.2. NMR spectra of 3

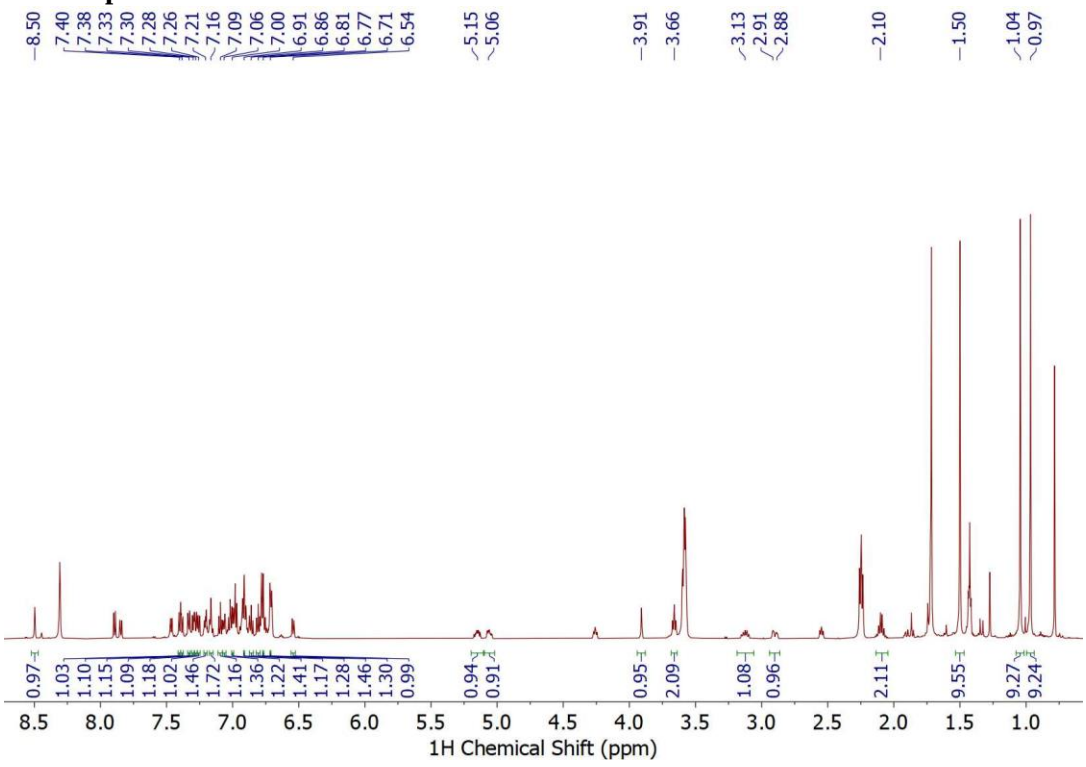


**Figure S8**. $^{1}H$ NMR spectrum of **3** (and **2** + 2,4-dihydroisoquinoline) ($C_6D_6$, 500 MHz, 25 °C).

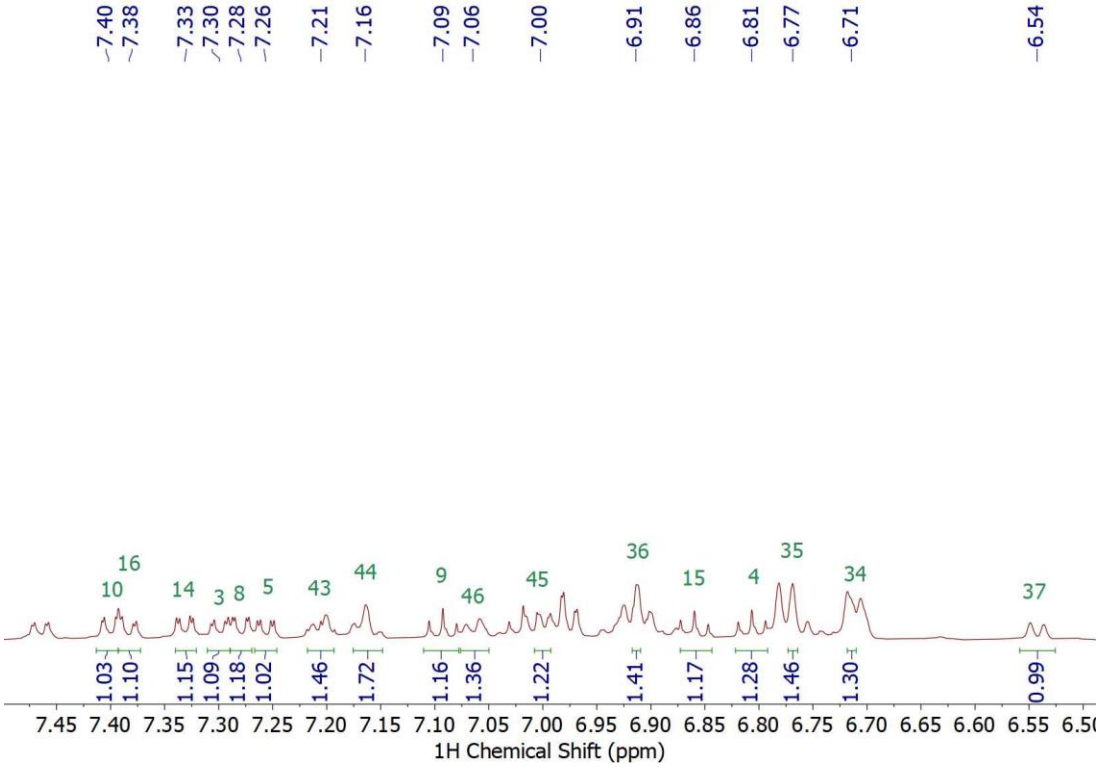


**Figure S9**. $^{1}$H NMR spectrum-expansion of **3** (and **2** + 2,4-dihydroisoquinoline) ($C_6D_6$, 500 MHz, 25 °C).

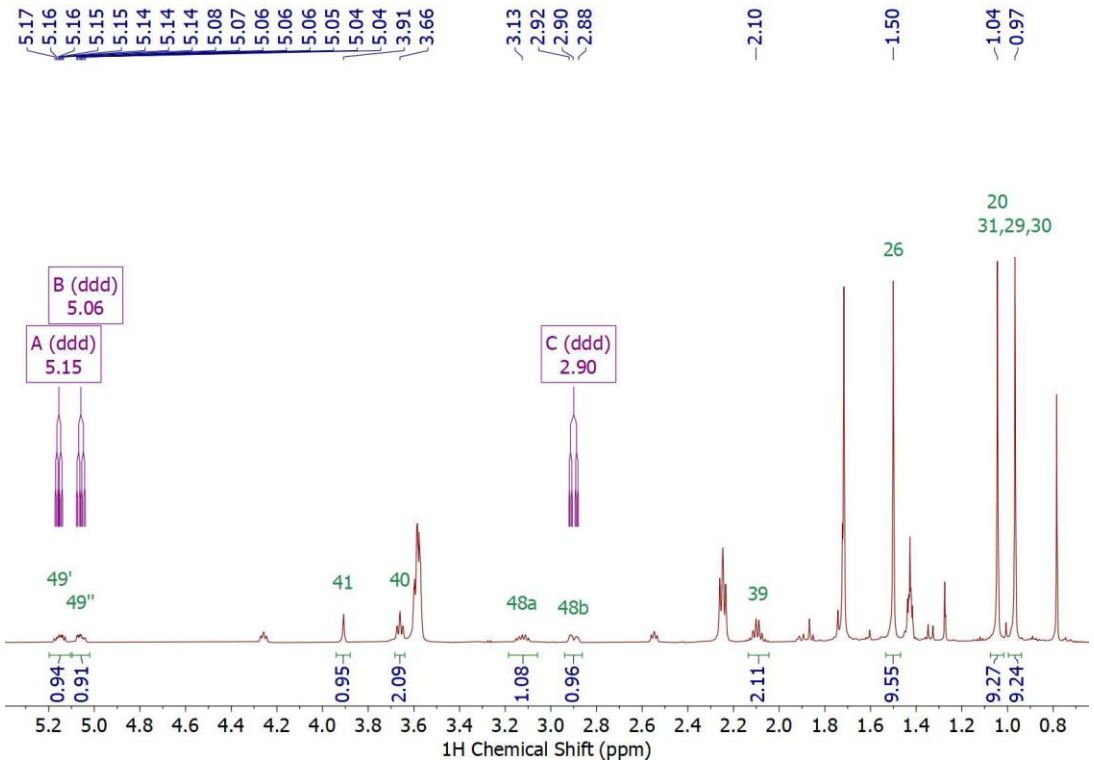


**Figure S10**. $^{1}$H NMR spectrum of **3** (and **2** + 2,4-dihydroisoquinoline) ($C_6D_6$, 500 MHz, 25 °C).

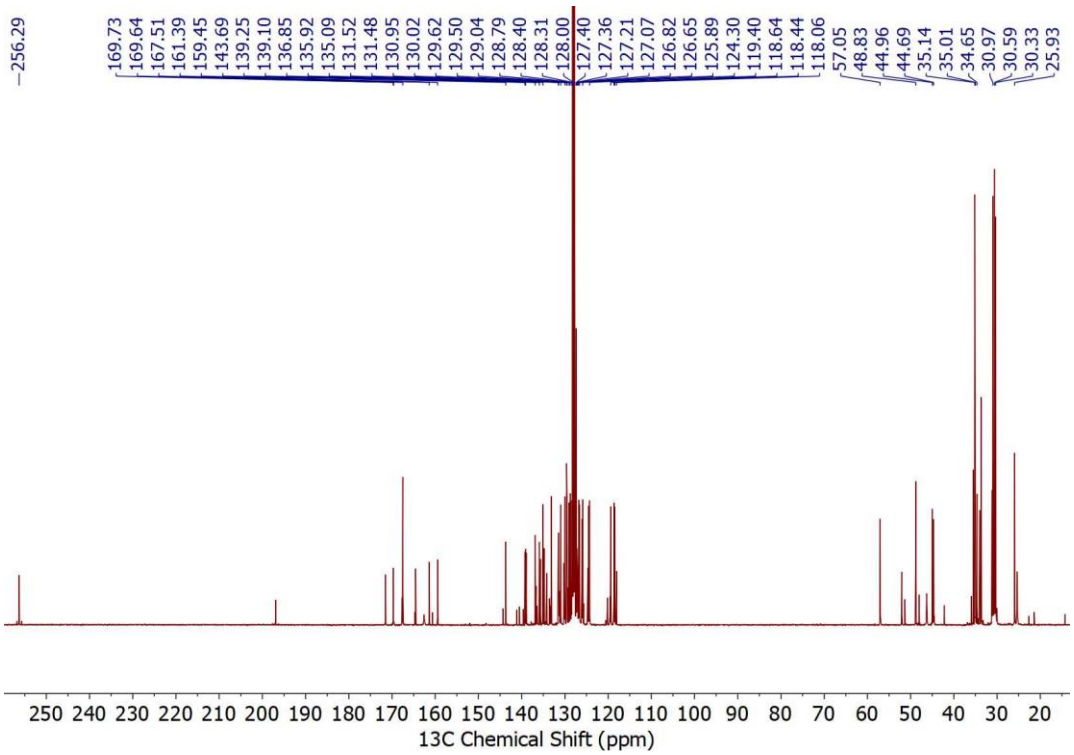


**Figure S11**. $^{13}C\{^{1}H\}$ NMR spectrum of **3** (and **2** + 2,4-dihydroisoquinoline) ($C_6D_6$, 500 MHz, 25 °C).-

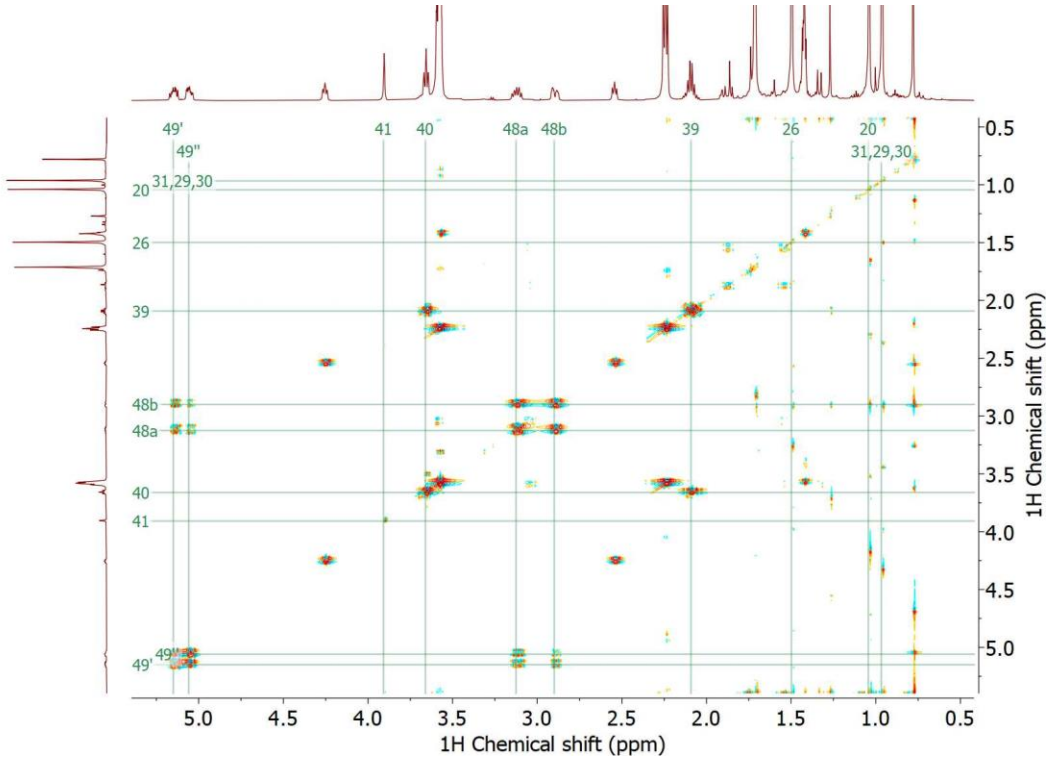


**Figure S12**. $^{1}H$-$^{1}H$ COSY NMR spectrum-expansion of **3** (and **2** + 2,4-dihydroisoquinoline) ($C_6D_6$, 500 MHz, 25 °C).

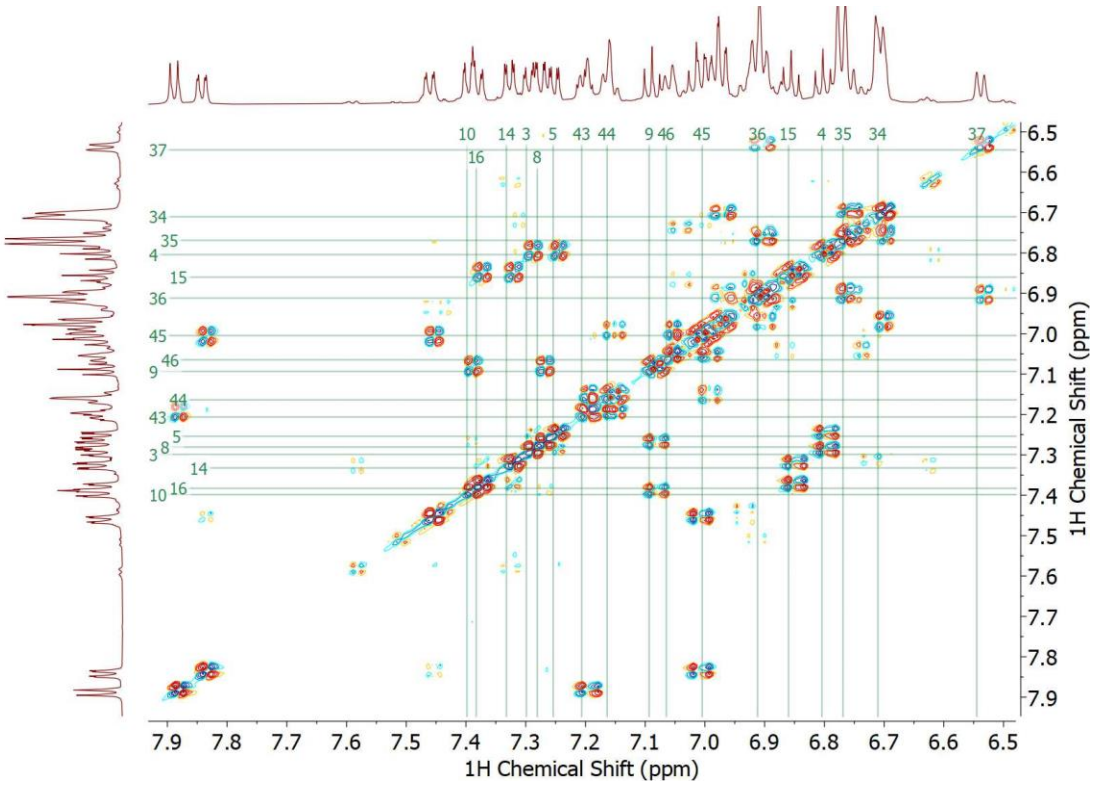


**Figure S13**. $^{1}$H-$^{1}$H COSY NMR spectrum-expansion of **3** (and **2** + 2,4-dihydroisoquinoline) ($C_6D_6$, 500 MHz, 25 °C).

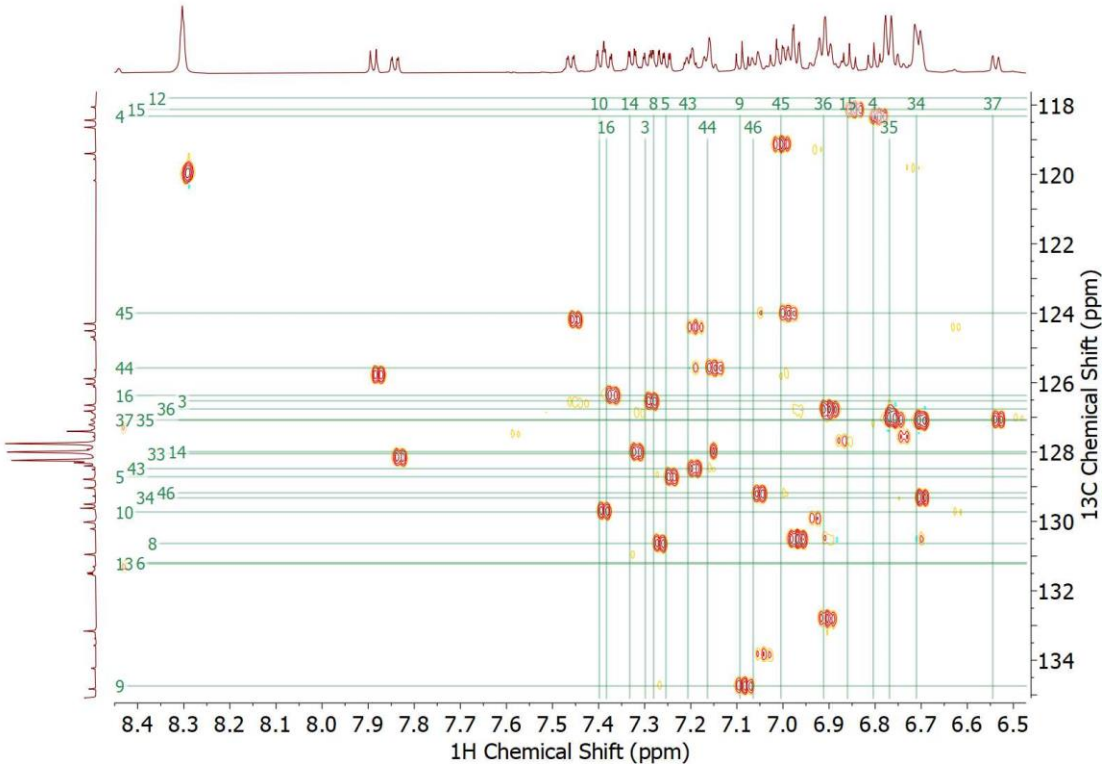


**Figure S14**. $^{1}$H-$^{13}$C HSQC NMR spectrum-expansion of **3** (and **2** + 2,4-dihydroisoquinoline) ($C_6D_6$, 500 MHz, 25 °C).

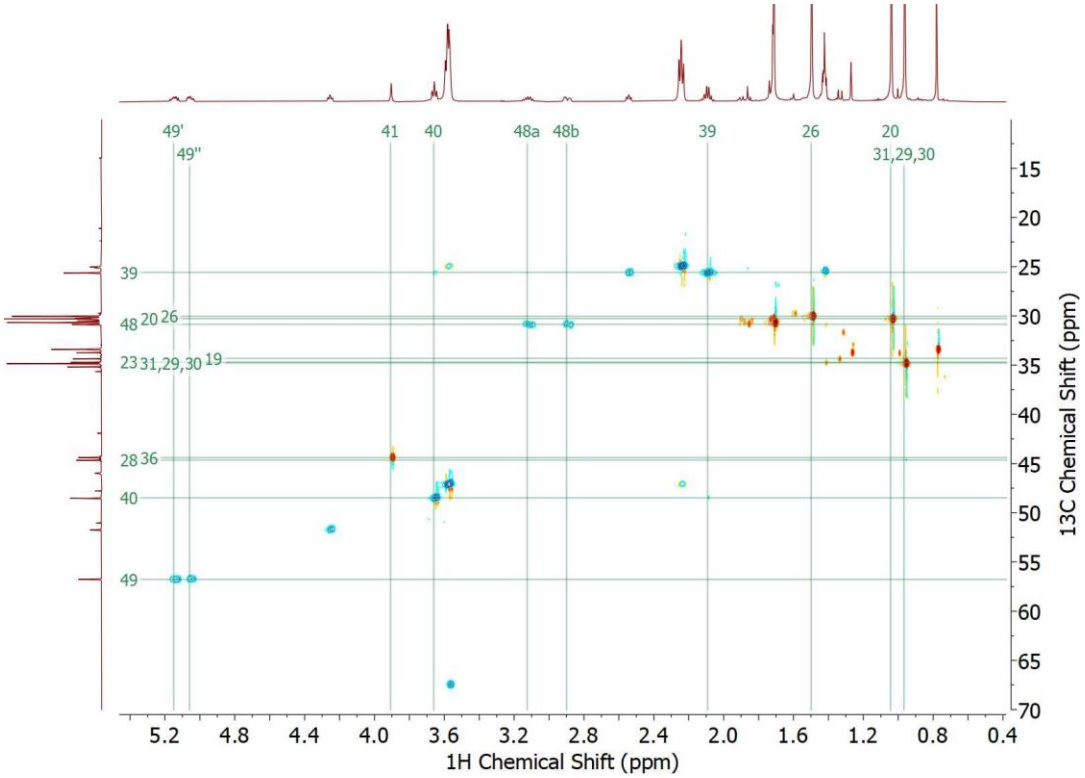


**Figure S15**. $^{1}H$-$^{13}C$ HSQC NMR spectrum-expansion of **3** (and **2** + 2,4-dihydroisoquinoline) ($C_6D_6$, 500 MHz, 25 °C).

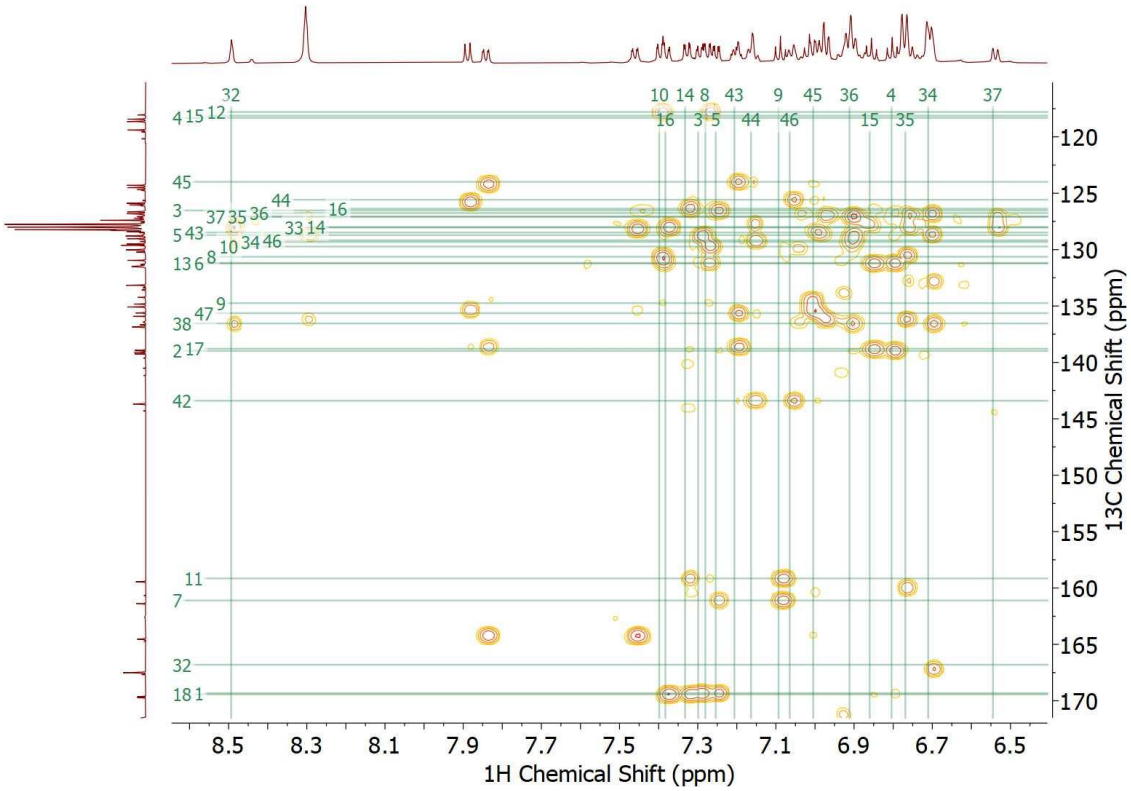


**Figure S16**. $^{1}H$-$^{13}C$ HMBC NMR spectrum-expansion of **3** (and **2** + 2,4-dihydroisoquinoline) ($C_6D_6$, 500 MHz, 25 °C).

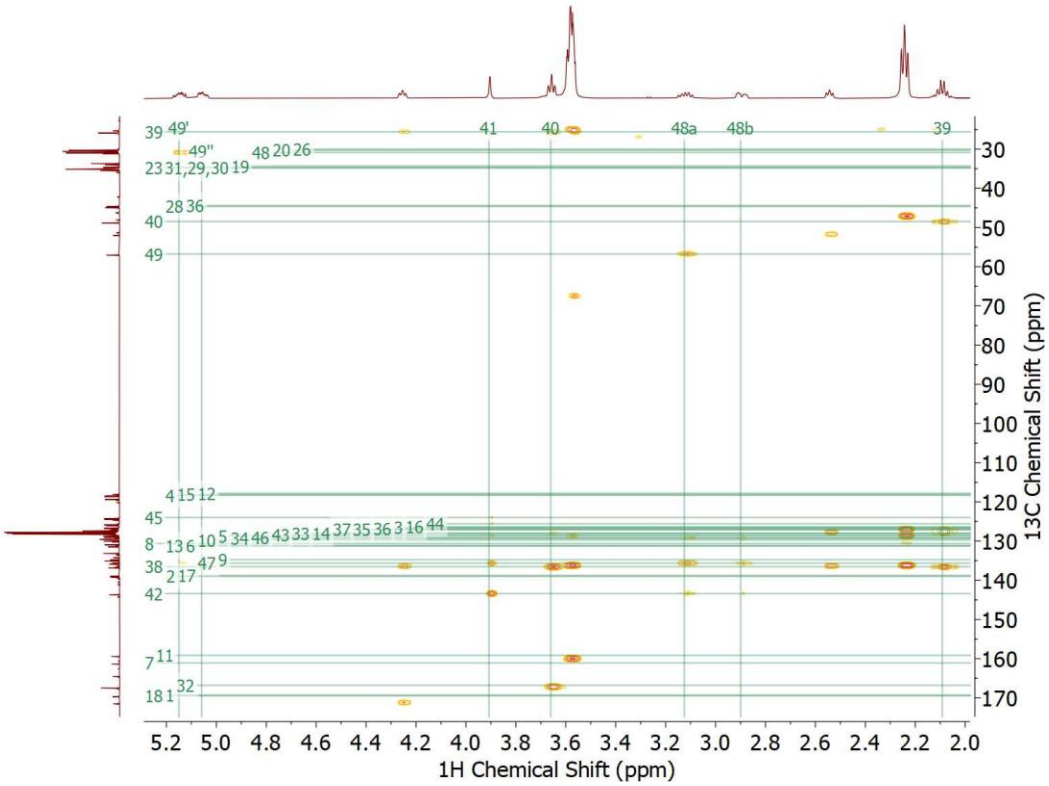


**Figure S17**. $^{1}H$-$^{13}C$ HMBC NMR spectrum-expansion of **3** (and **2** + 2,4-dihydroisoquinoline) ($C_6D_6$, 500 MHz, 25 °C).

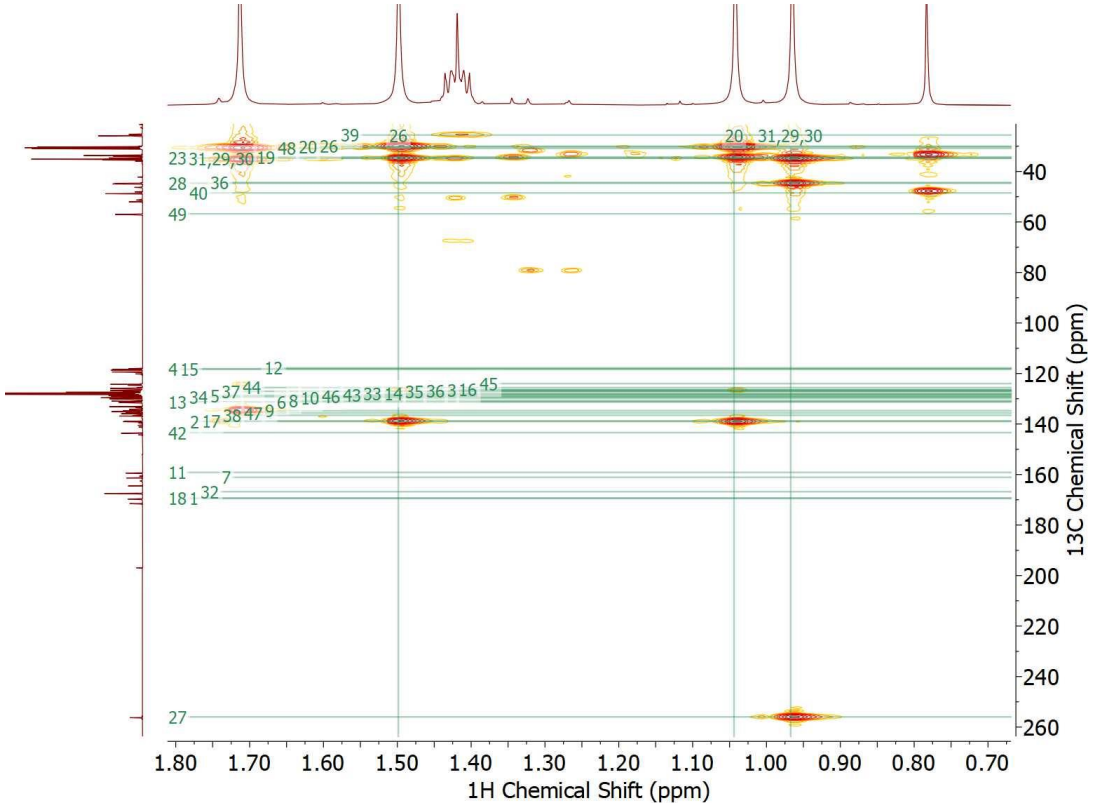


**Figure S18**. $^{1}H$-$^{13}C$ HMBC NMR spectrum-expansion of **3** (and **2** + 2,4-dihydroisoquinoline) ($C_6D_6$, 500 MHz, 25 °C).

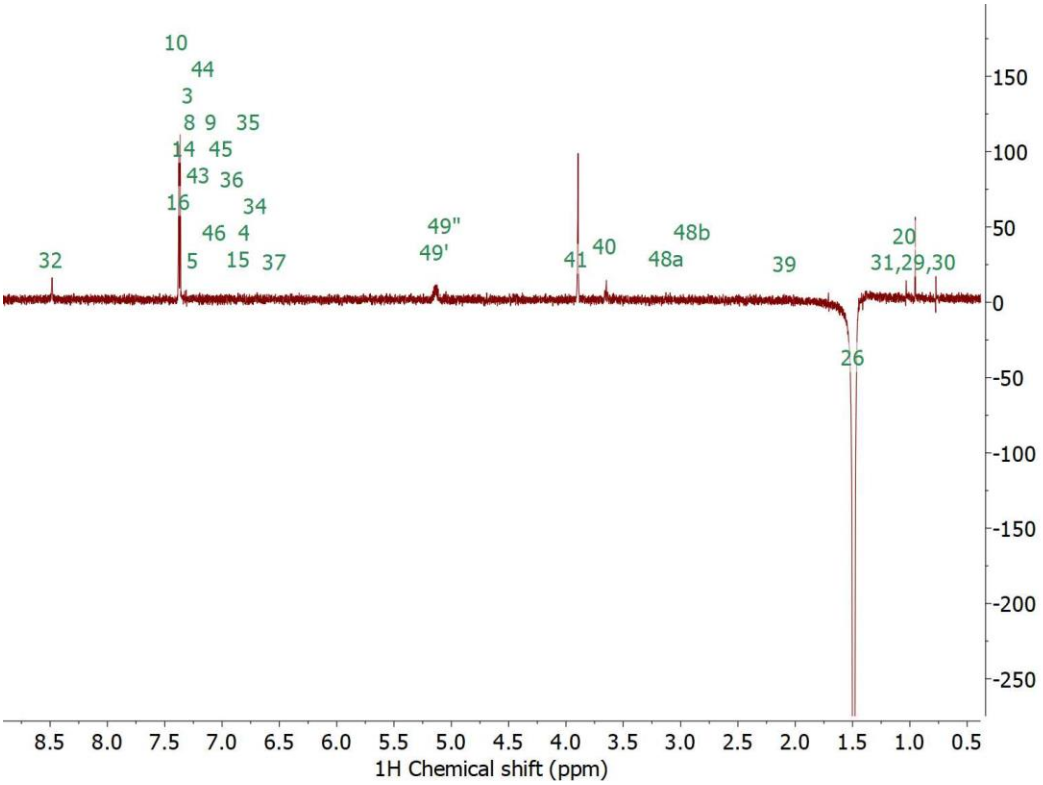


**Figure S19**. 1D gNOESY spectrum of **3** (and **2** + 2,4-dihydroisoquinoline), collected on $H_{24\text{-}26}$ ($C_6D_6$, 500 MHz, 25 °C).

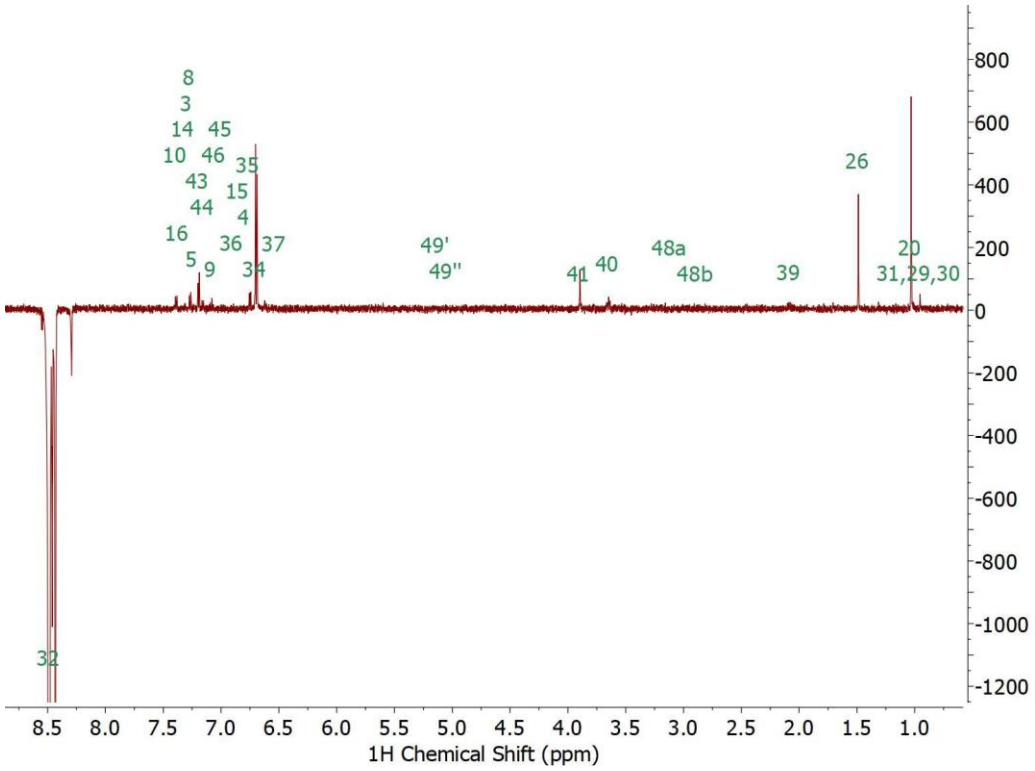


**Figure S20**. 1D gNOESY spectrum of **3** (and **2** + 2,4-dihydroisoquinoline), collected on $H_{32}$ ($C_6D_6$, 500 MHz, 25 °C).

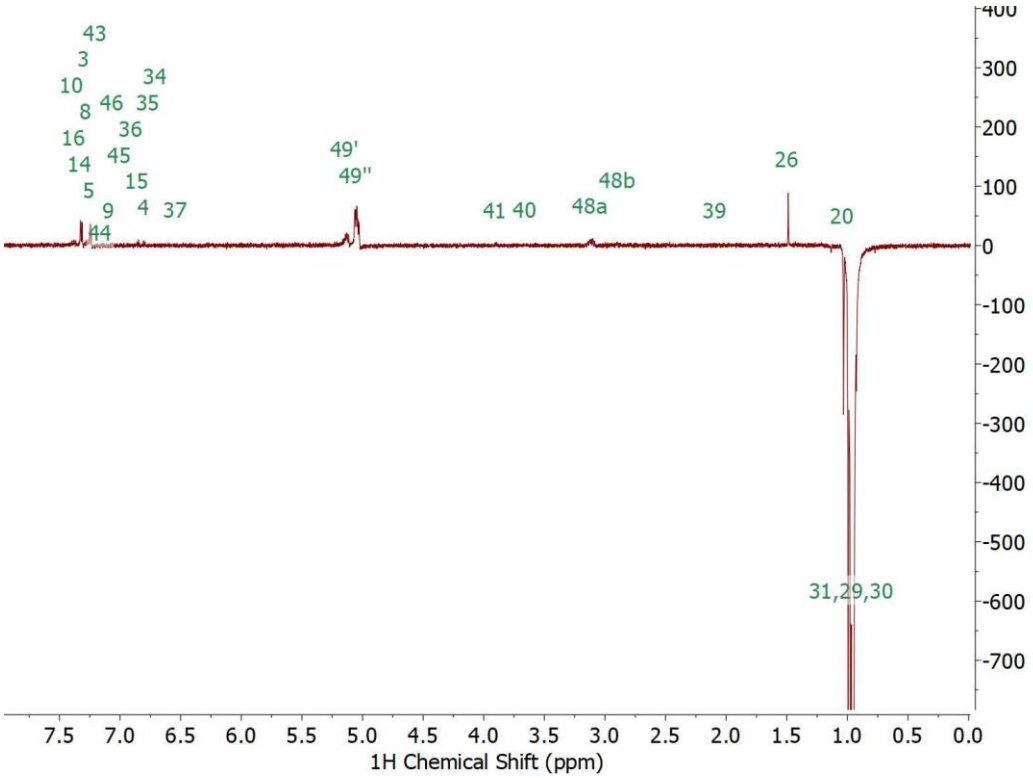


**Figure S21**. 1D gNOESY spectrum of **3** (and **2** + 2,4-dihydroisoquinoline), collected on $H_{29\text{-}31}$ ($C_6D_6$, 500 MHz, 25 °C).

### 3.3. NMR spectra of 4-Me

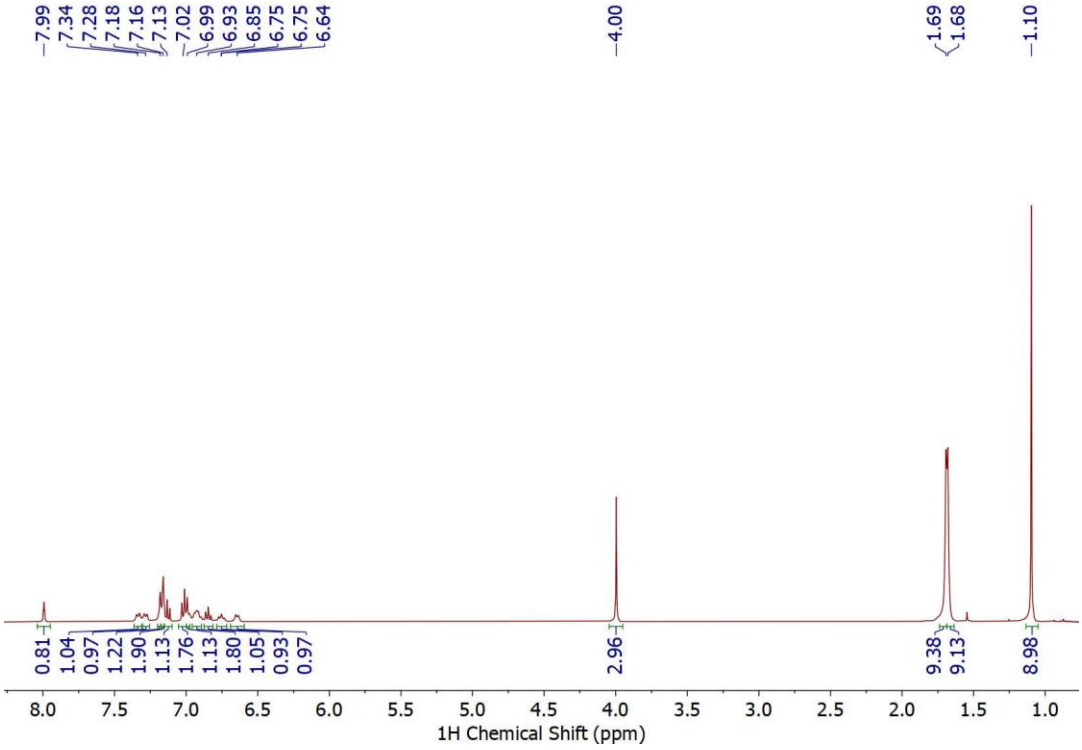


**Figure S22**. $^1$H NMR spectrum of **4-Me** ($C_6D_6$, 500 MHz, 25 °C).

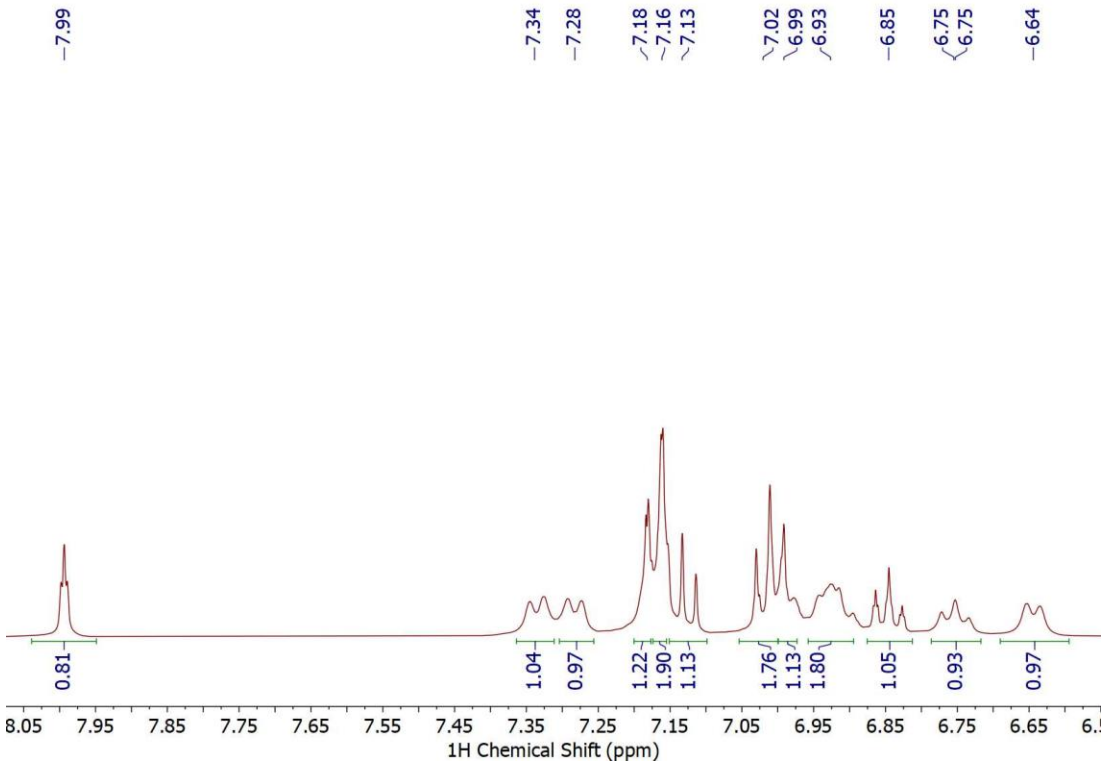


**Figure S23**. $^{1}H$ NMR spectrum-expansion of **4-Me** ($C_6D_6$, 500 MHz, 25 °C).

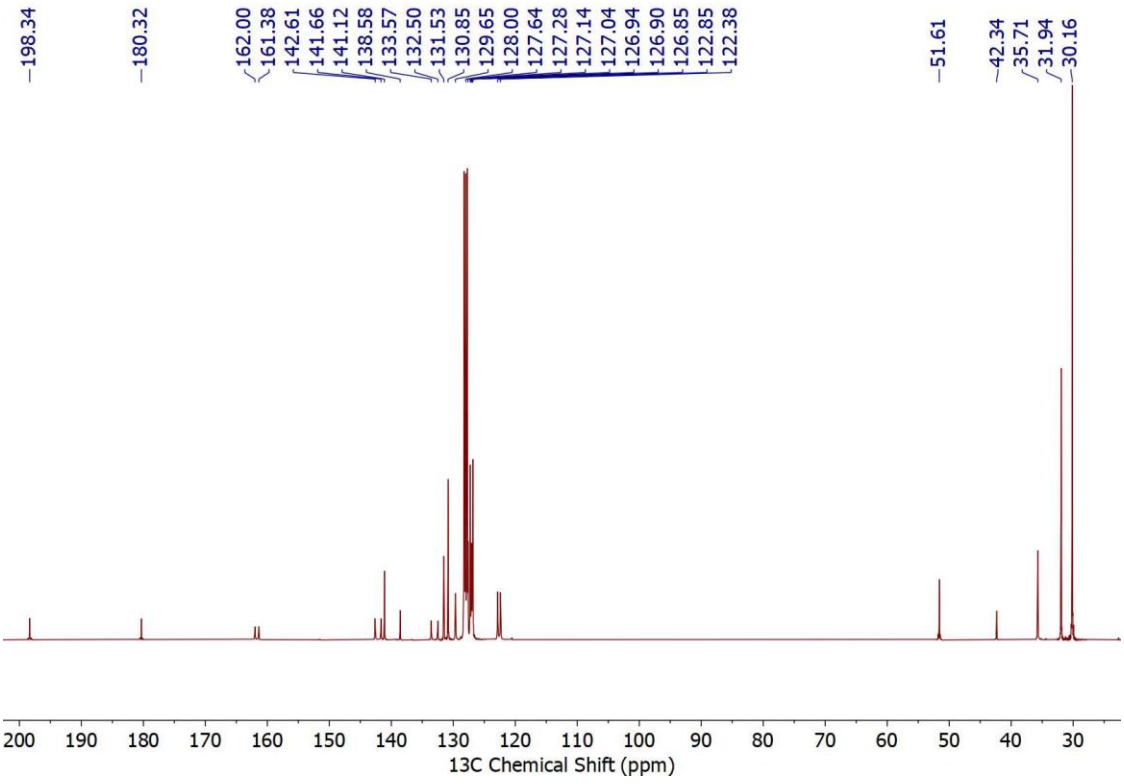


**Figure S24**. $^{13}C\{^{1}H\}$ NMR spectrum of **4-Me** ($C_6D_6$, 500 MHz, 25 °C).

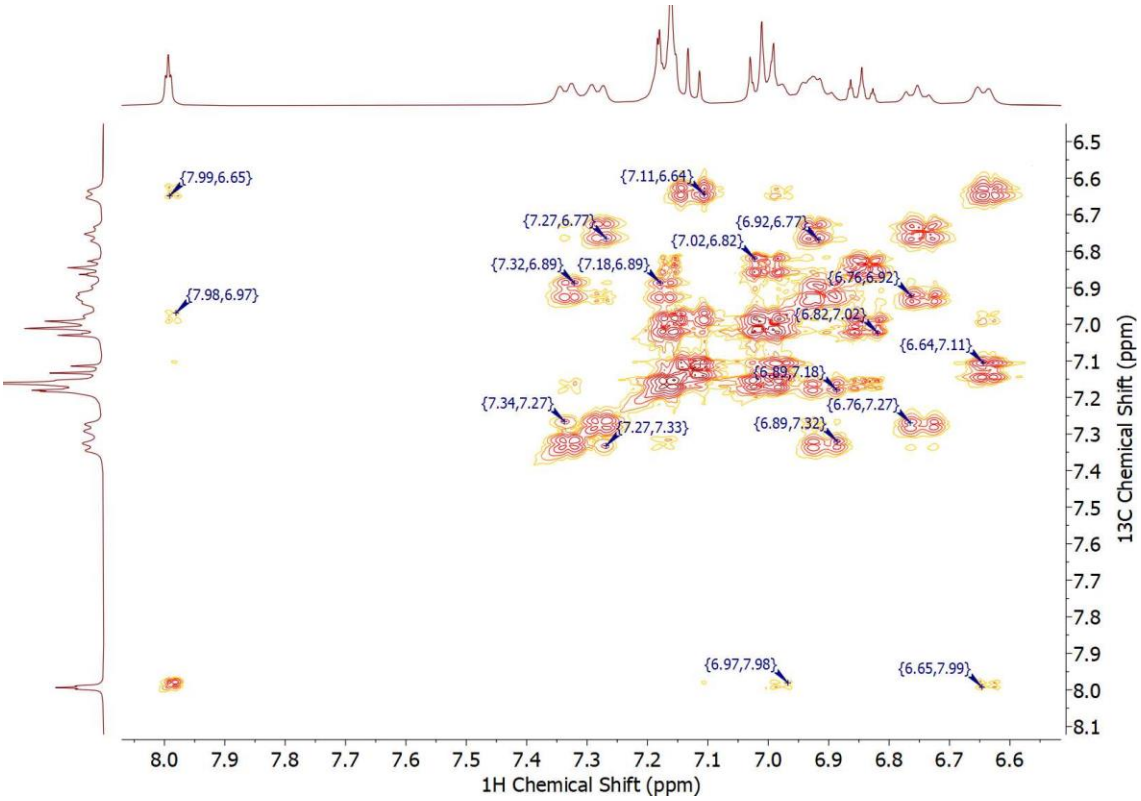


**Figure S25**. $^{1}$H-$^{1}$H COSY NMR spectrum-expansion of **4-Me** ($C_6D_6$, 500 MHz, 25 °C).

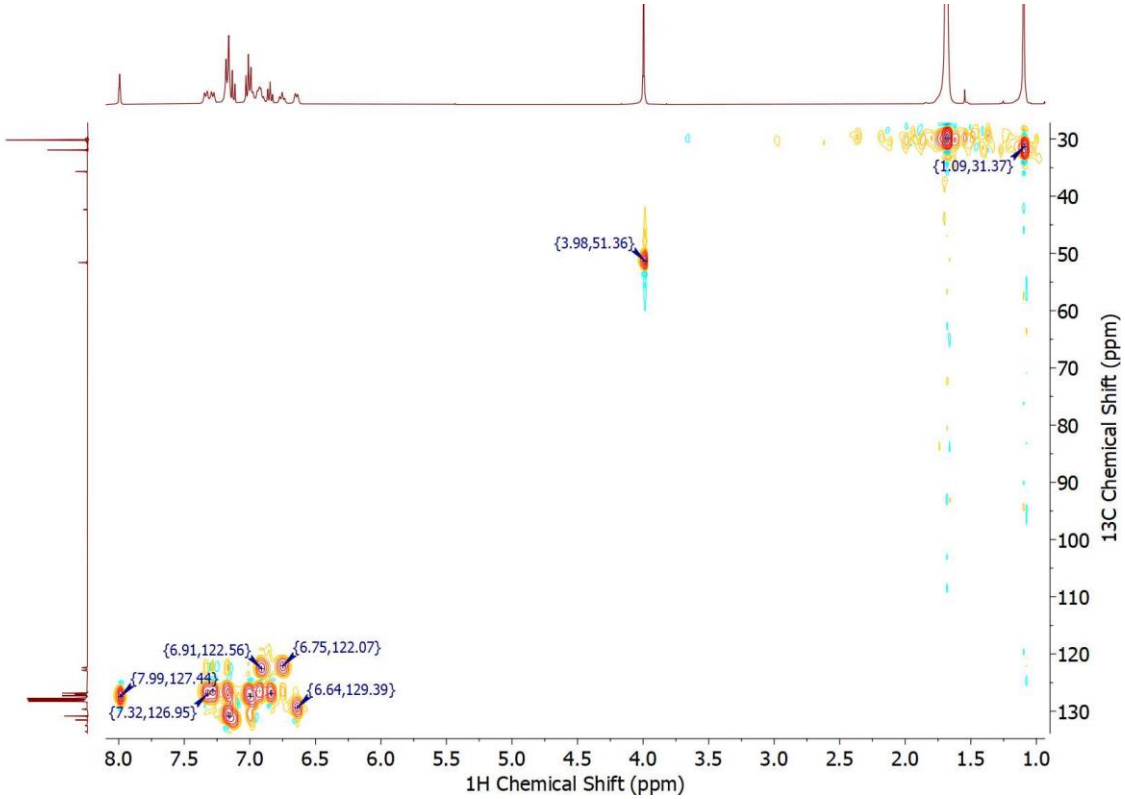


**Figure S26**. $^{1}$H-$^{13}$C HSQC NMR spectrum of **4-Me** ($C_6D_6$, 500 MHz, 25 °C).

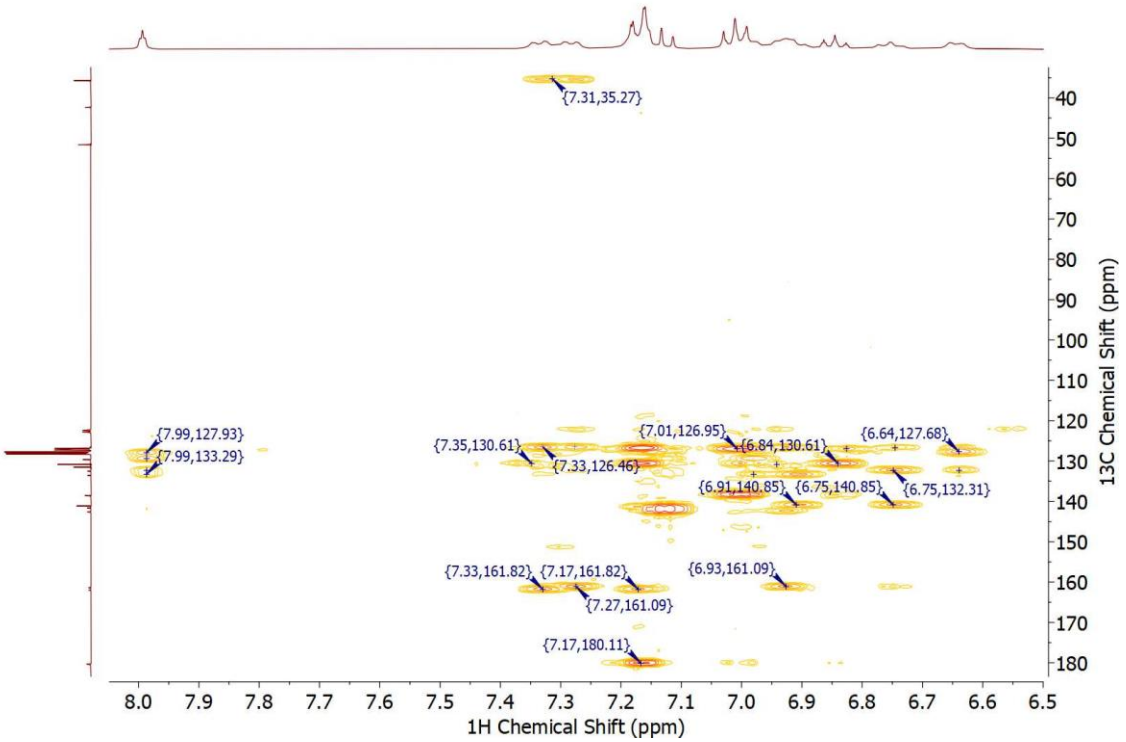


**Figure S27**. $^{1}H$-$^{13}C$ HMBC NMR spectrum-expansion of **4-Me** ($C_6D_6$, 500 MHz, 25 °C).

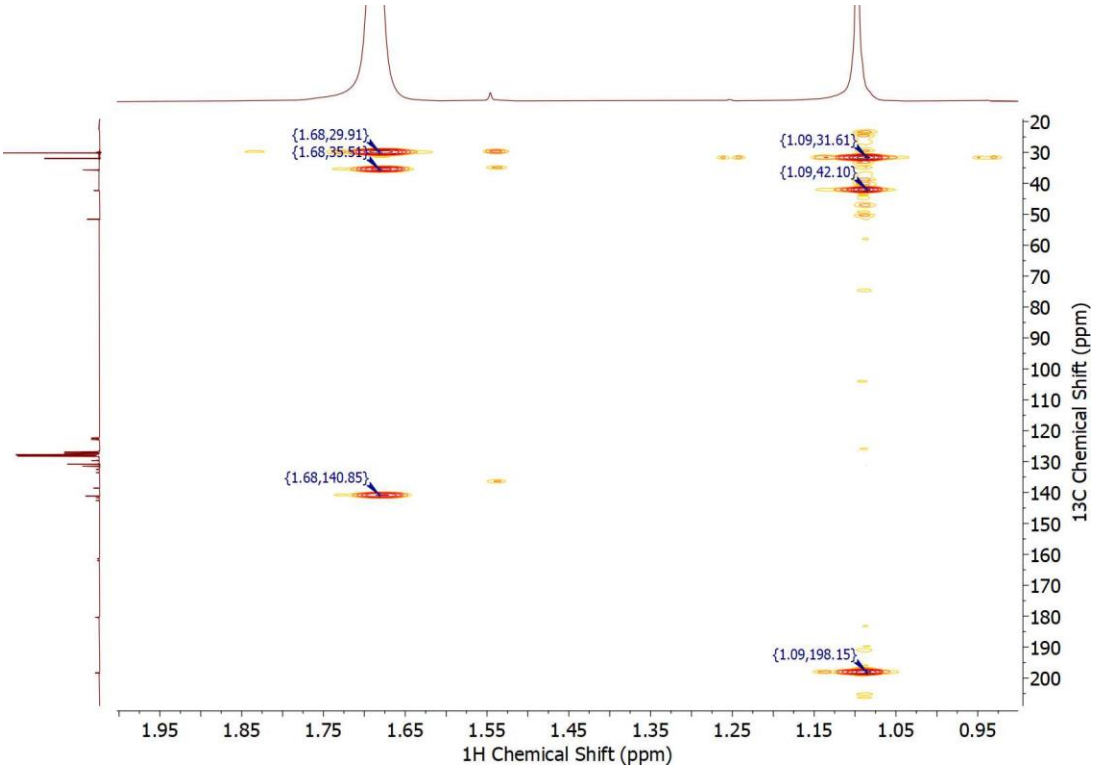


**Figure S28**. $^{1}H$-$^{13}C$ HMBC NMR spectrum-expansion of **4-Me** ($C_6D_6$, 500 MHz, 25 °C).

## 3.4. NMR spectra of 4-TMS

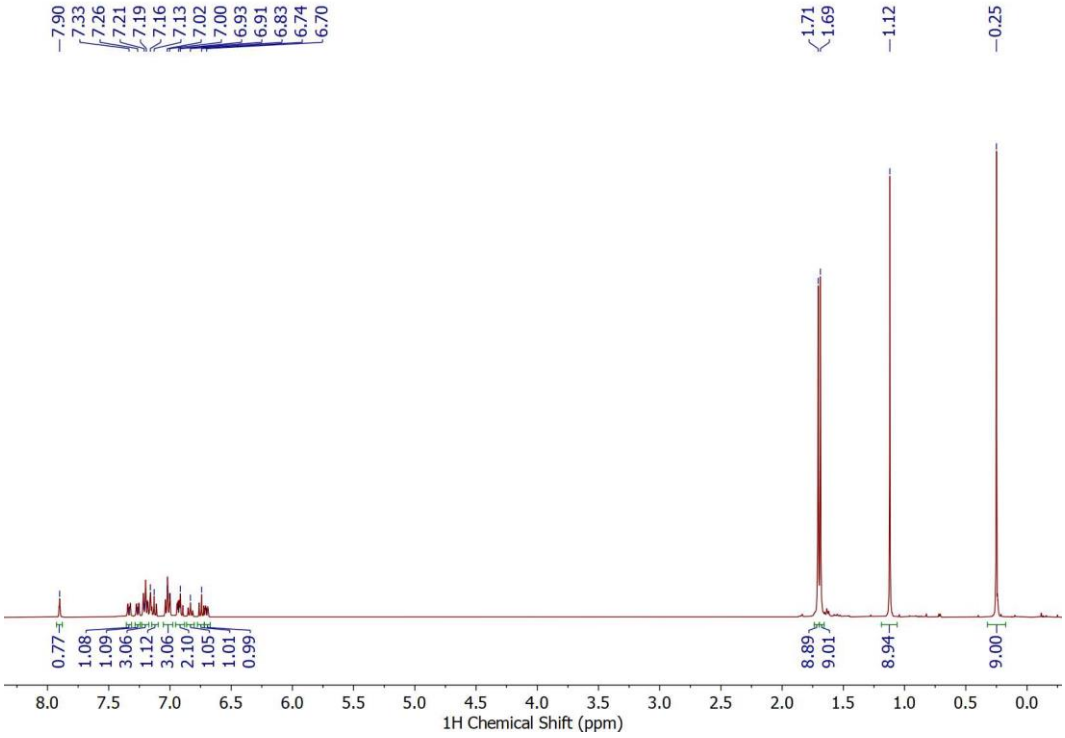


**Figure S29**. $^{1}$H NMR spectrum of **4-TMS** ($C_6D_6$, 400 MHz, 25 °C).

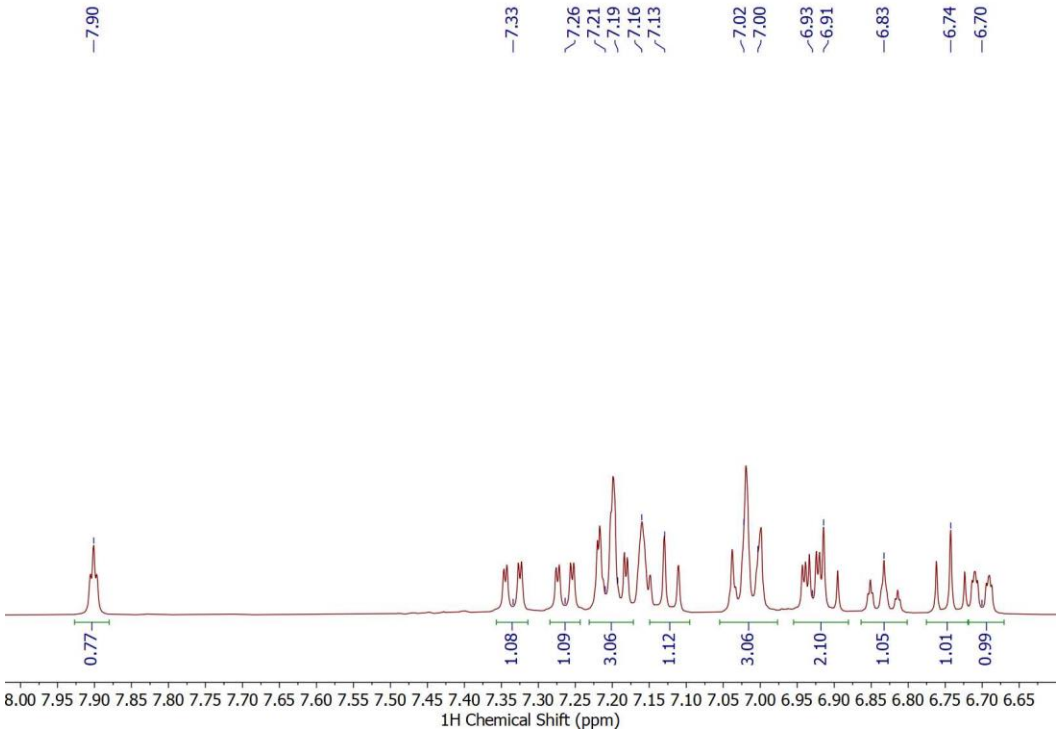


**Figure S30**. $^{1}$H NMR spectrum-expansion of **4-Me** ($C_6D_6$, 400 MHz, 25 °C).

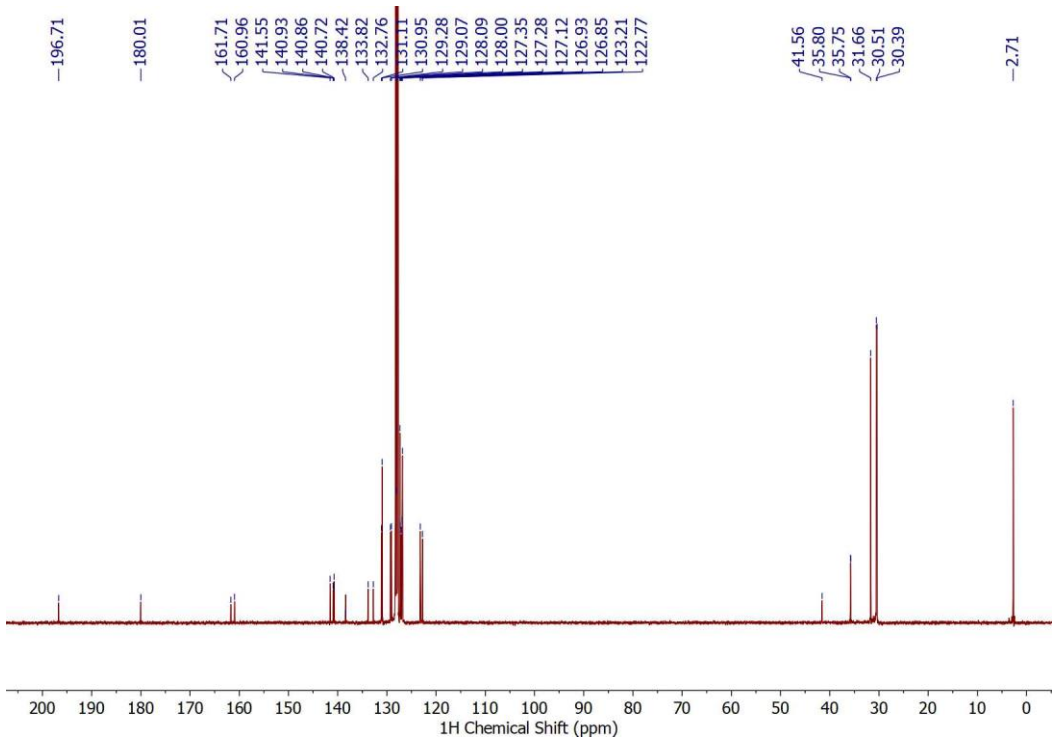


**Figure S31**. $^{13}C\{^{1}H\}$ NMR spectrum of **4-Me** ($C_6D_6$, 400 MHz, 25 °C).

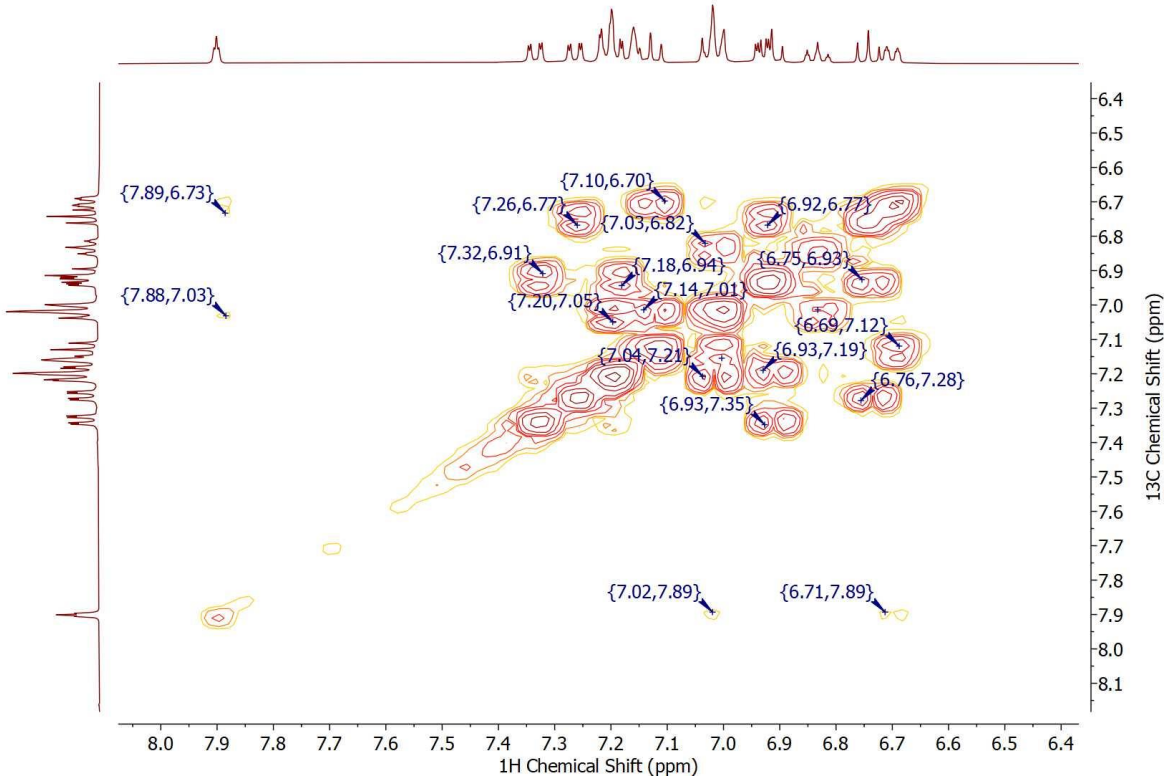


**Figure S32**. $^{1}H$-$^{1}H$ COSY NMR spectrum-expansion of **4-Me** ($C_6D_6$, 400 MHz, 25 °C).

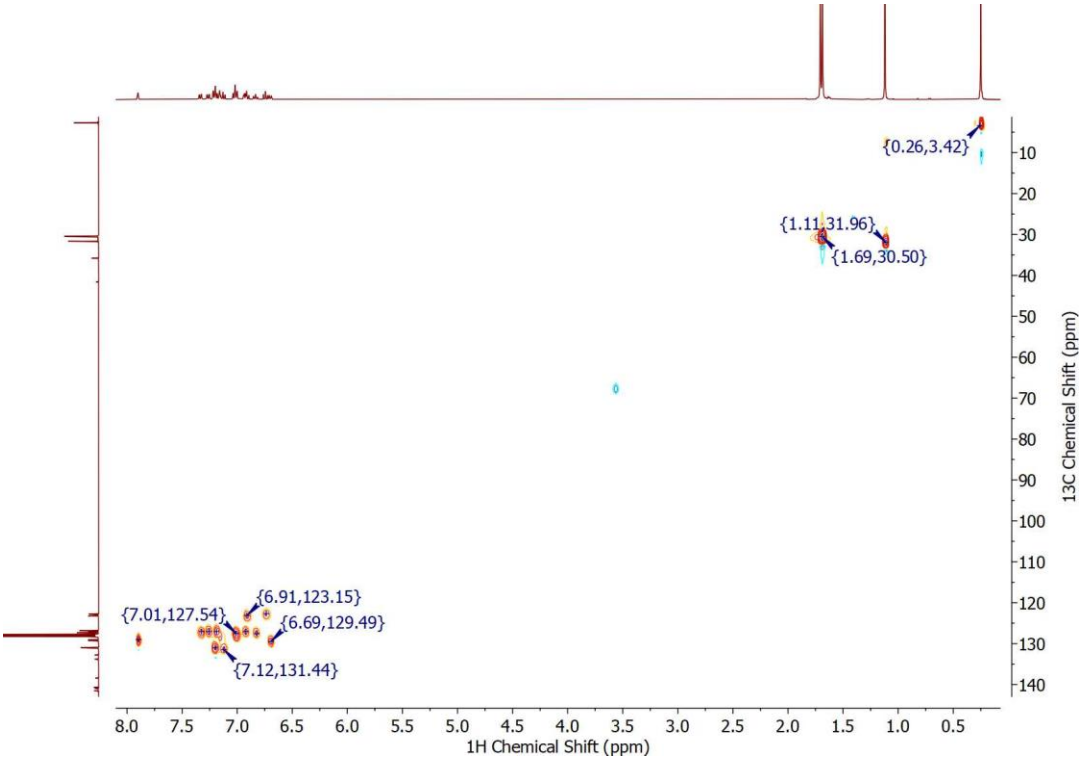


**Figure S33**. $^{1}H$-$^{13}C$ HSQC NMR spectrum of **4-Me** ($C_6D_6$, 400 MHz, 25 °C).

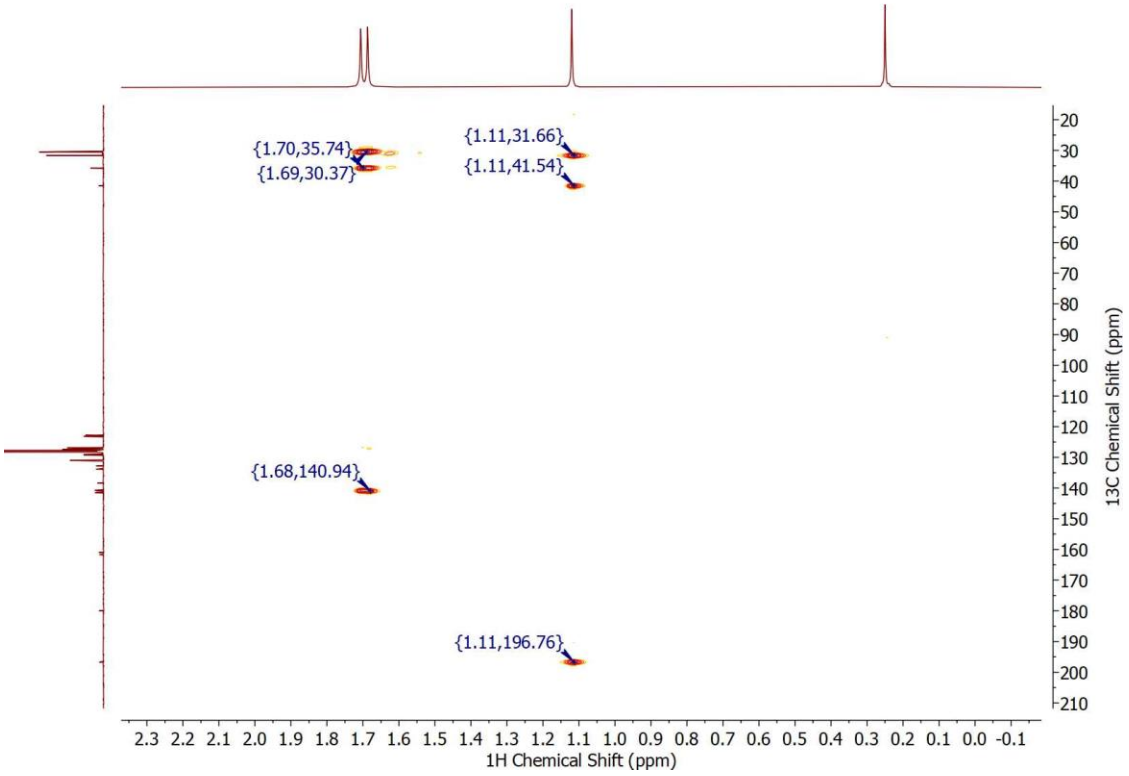


**Figure S34**. $^{1}H$-$^{13}C$ HMBC NMR spectrum-expansion of **4-Me** ($C_6D_6$, 400 MHz, 25 °C).

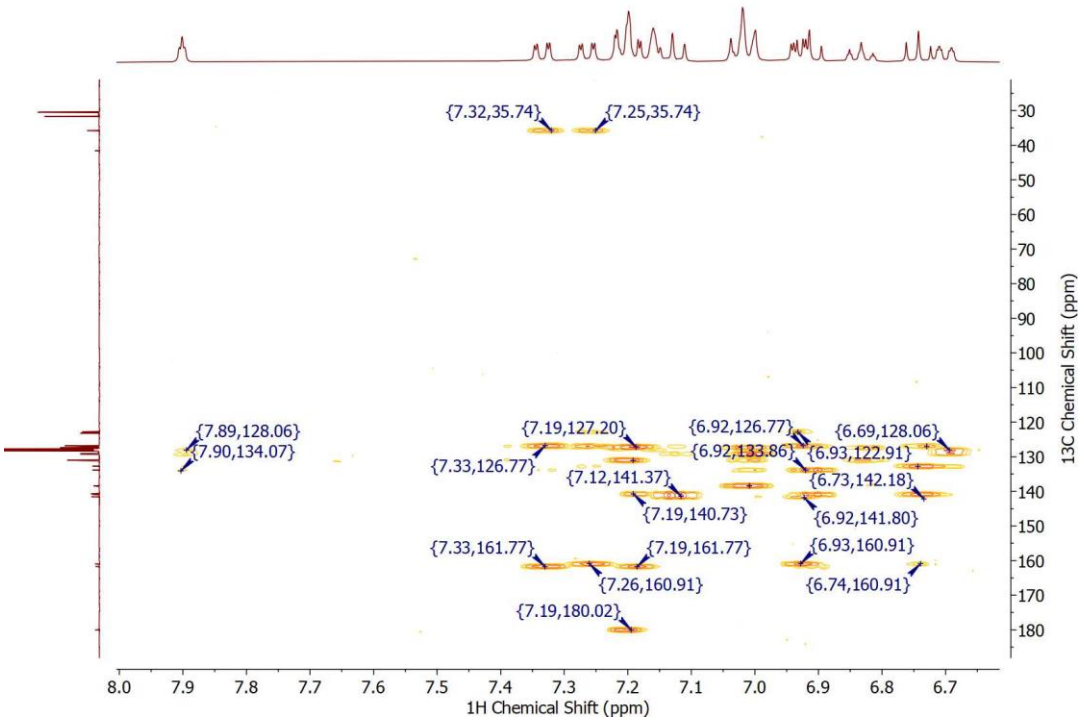


**Figure S35**. $^{1}H$-$^{13}C$ HMBC NMR spectrum-expansion of **4-Me** ($C_6D_6$, 400 MHz, 25 °C).

## 3.5. NMR spectra of 4-Ph

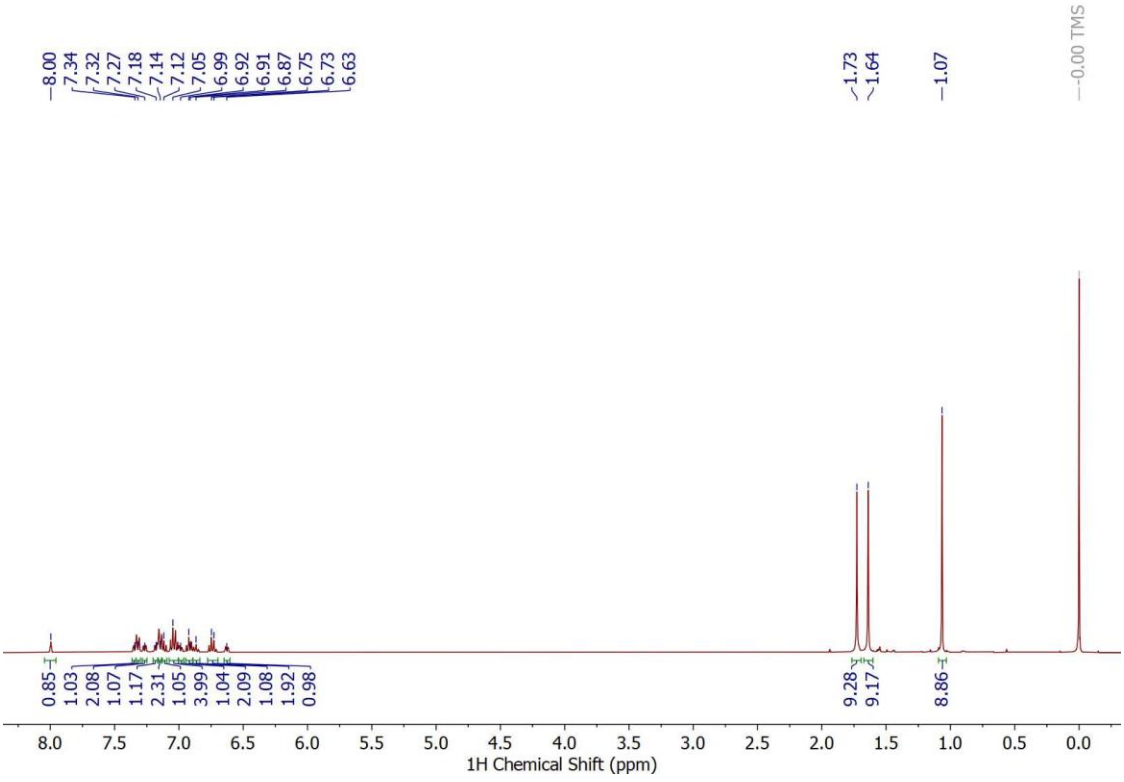


**Figure S36**. $^{1}H$ NMR spectrum of **4-Ph** ($C_6D_6$, 400 MHz, 25 °C).

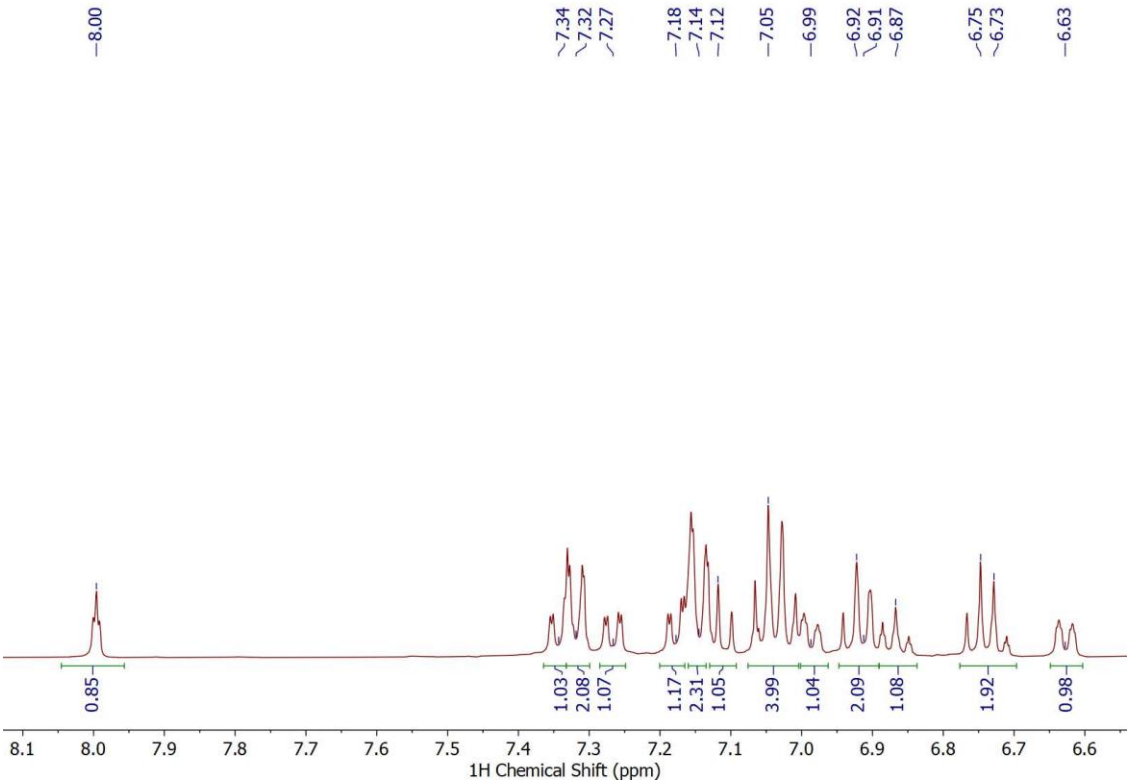


**Figure S37**. $^{1}H$ NMR spectrum-expansion of **4-Ph** ($C_6D_6$, 400 MHz, 25 °C).

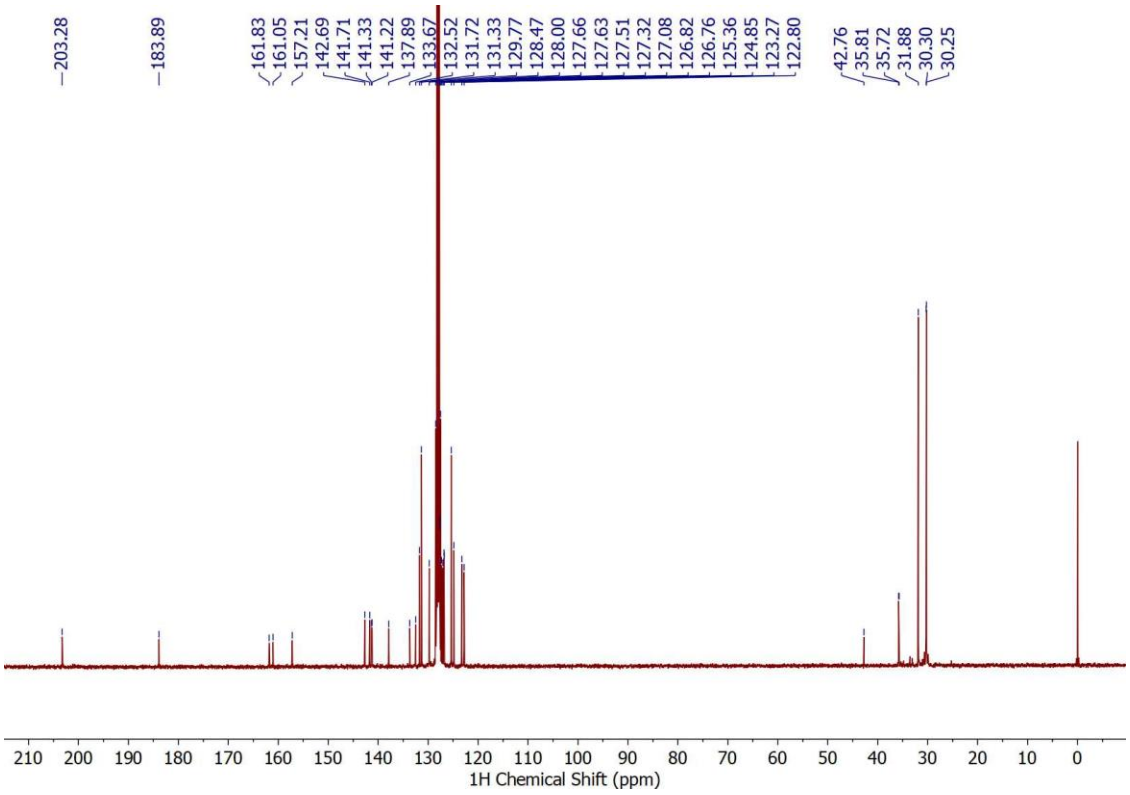


**Figure S38**. $^{13}C\{^{1}H\}$ NMR spectrum of **4-Ph** ($C_6D_6$, 400 MHz, 25 °C).

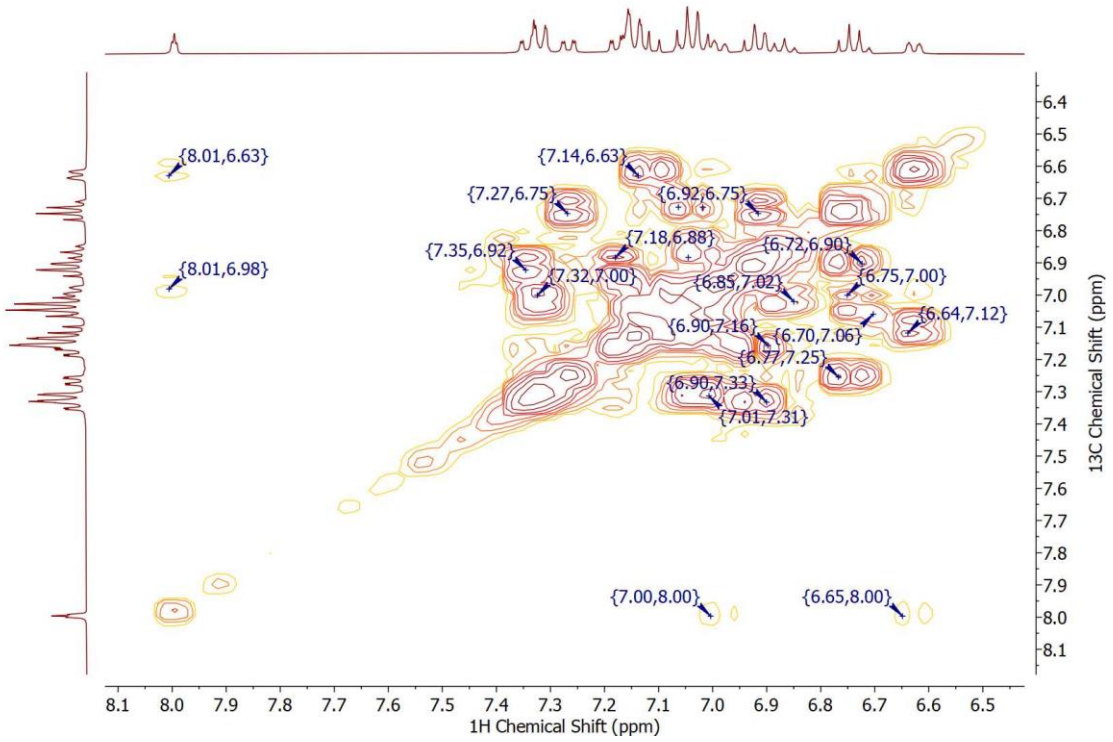


**Figure S39**. $^{1}$H-$^{1}$H COSY NMR spectrum-expansion of **4-Ph** ($C_6D_6$, 400 MHz, 25 °C).

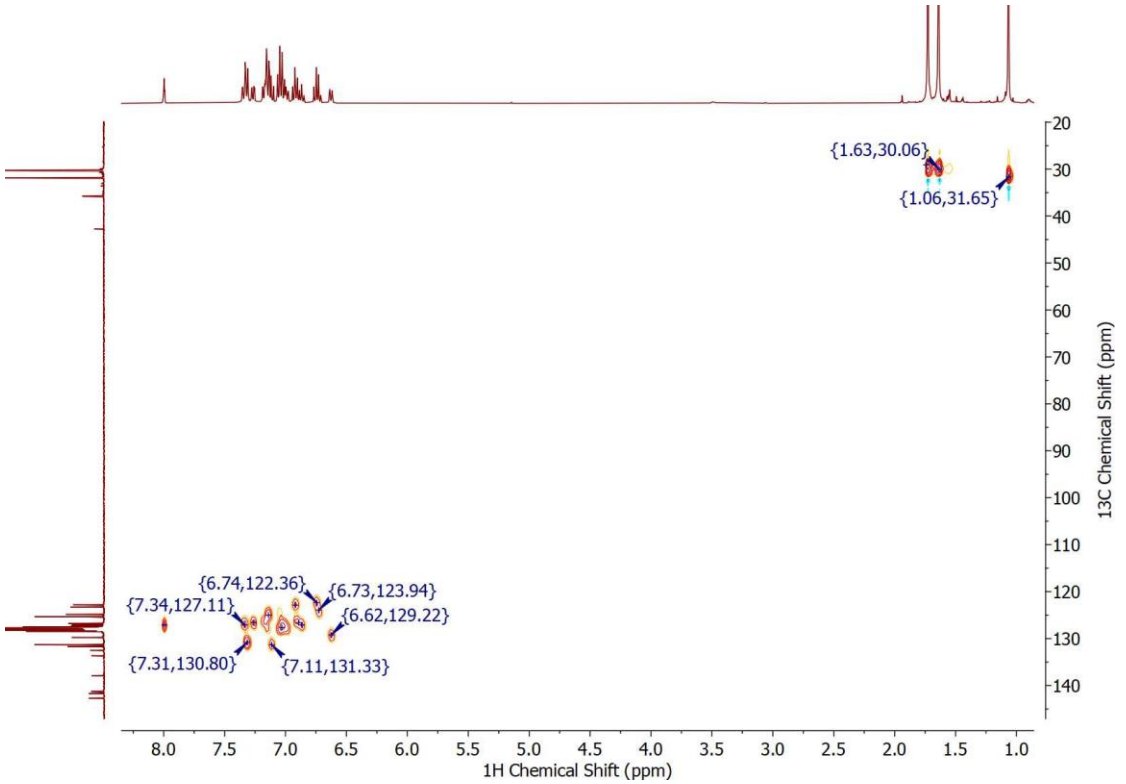


**Figure S40**. $^{1}$H-$^{13}$C HSQC NMR spectrum of **4-Ph** ($C_6D_6$, 400 MHz, 25 °C).

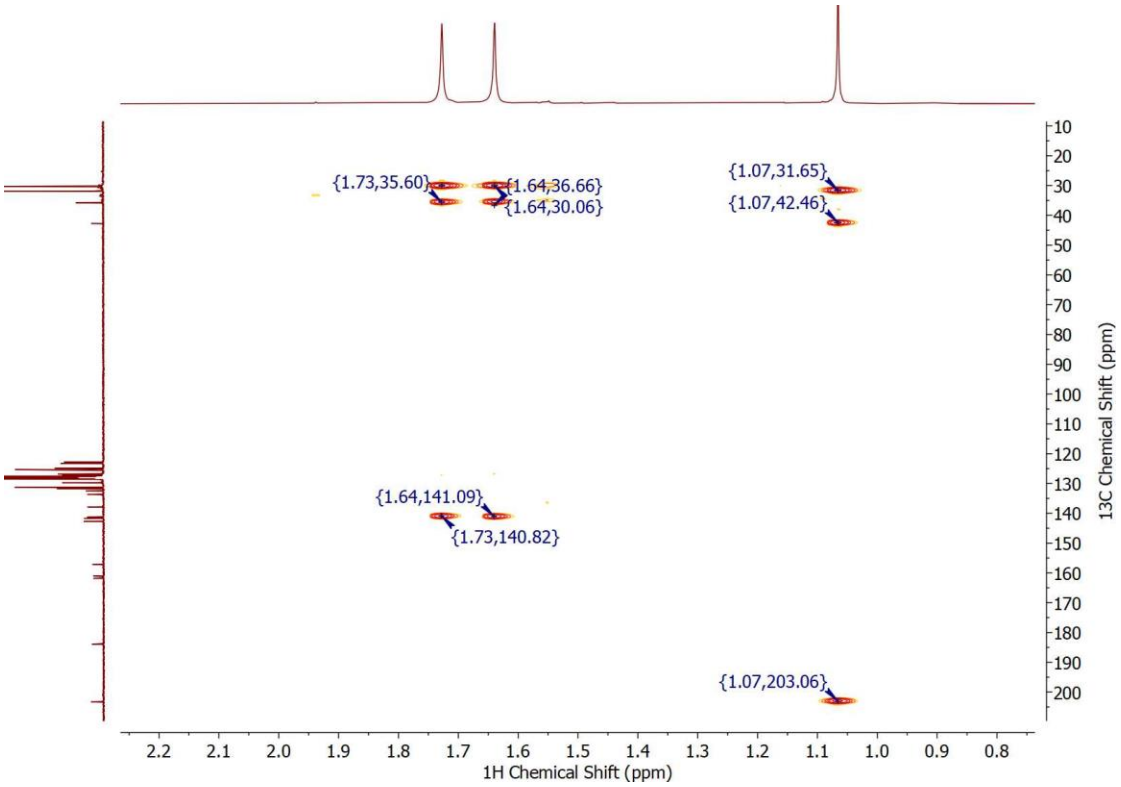


**Figure S41**. $^{1}H$-$^{13}C$ HMBC NMR spectrum-expansion of **4-Ph** ($C_6D_6$, 400 MHz, 25 °C).

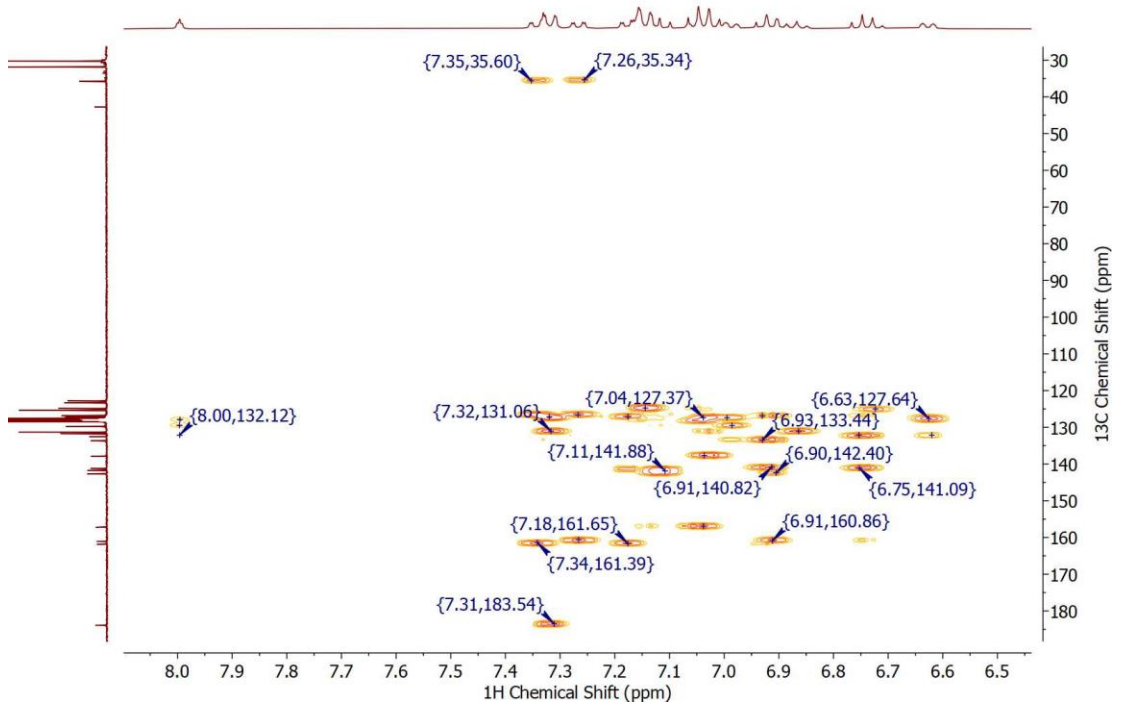


**Figure S42**. $^{1}H$-$^{13}C$ NMR HMBC spectrum-expansion of **4-Ph** ($C_6D_6$, 400 MHz, 25 °C).

### 3.6. NMR spectra of 4-Bn

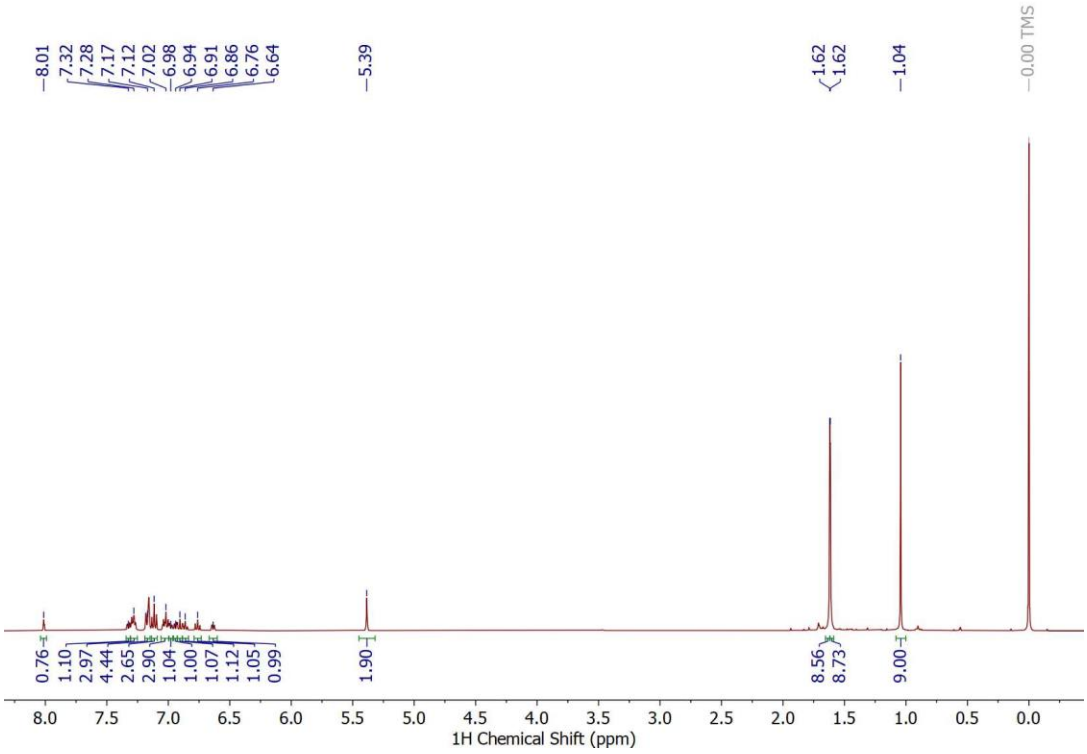


**Figure S43**. $^{1}$H NMR spectrum of **4-Bn** ($C_6D_6$, 400 MHz, 25 °C).

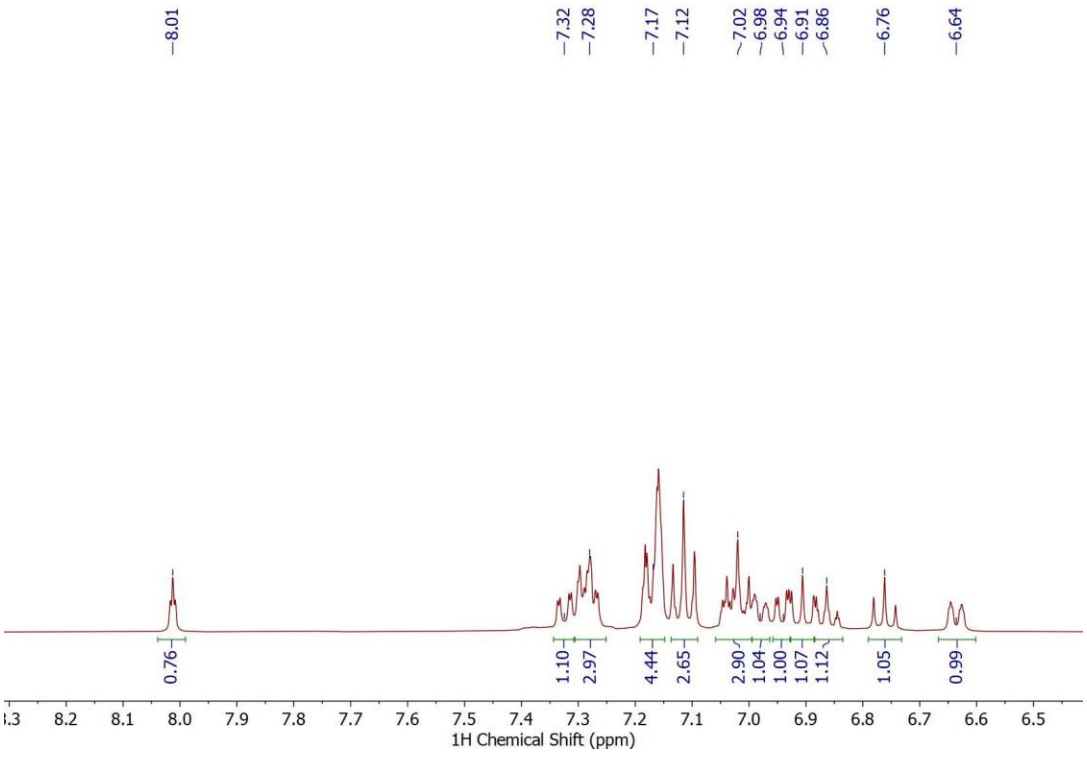


**Figure S44**. $^{1}$H NMR spectrum-expansion of **4-Bn** ($C_6D_6$, 400 MHz, 25 °C).

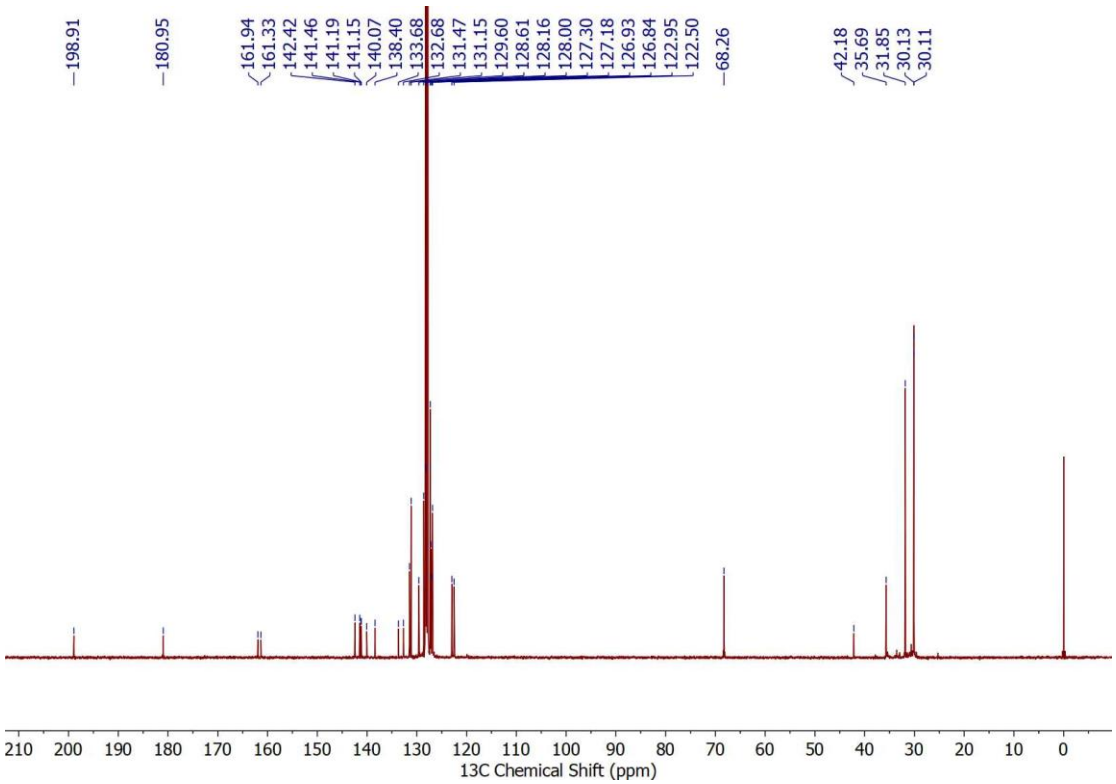


**Figure S45**. $^{13}C\{^{1}H\}$ NMR spectrum of **4-Bn** ($C_6D_6$, 400 MHz, 25 °C).

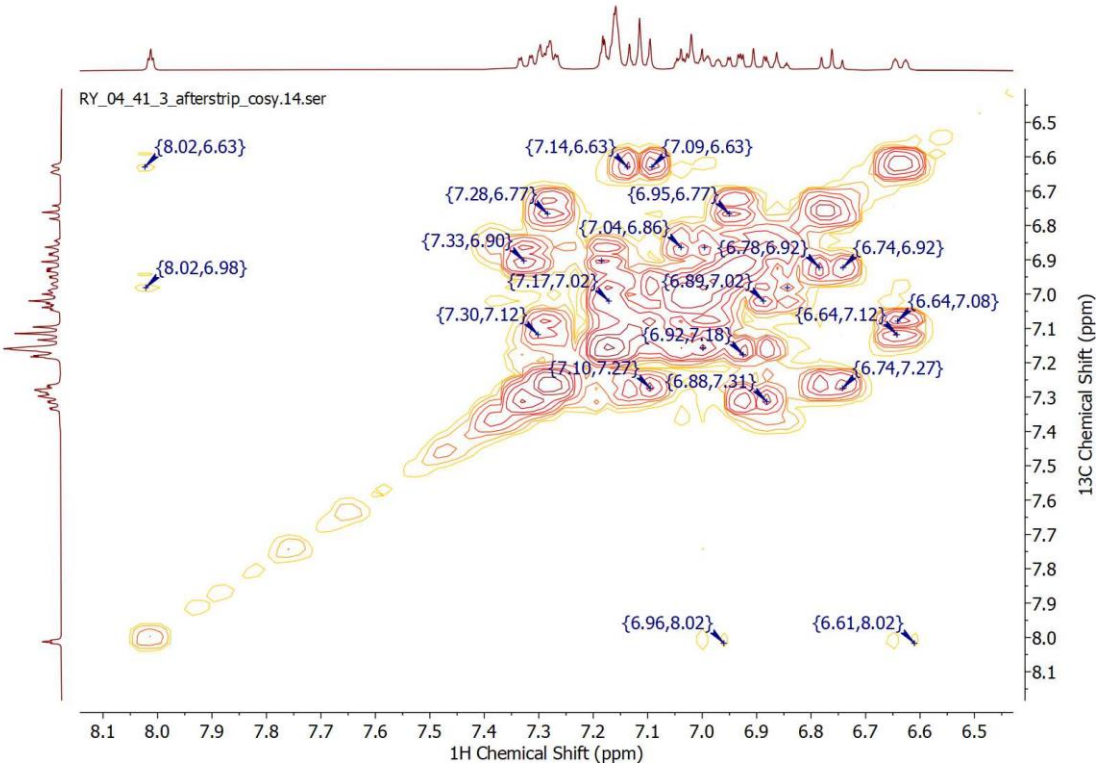


**Figure S46**. $^{1}H$-$^{1}H$ COSY NMR spectrum-expansion of **4-Bn** ($C_6D_6$, 400 MHz, 25 °C).

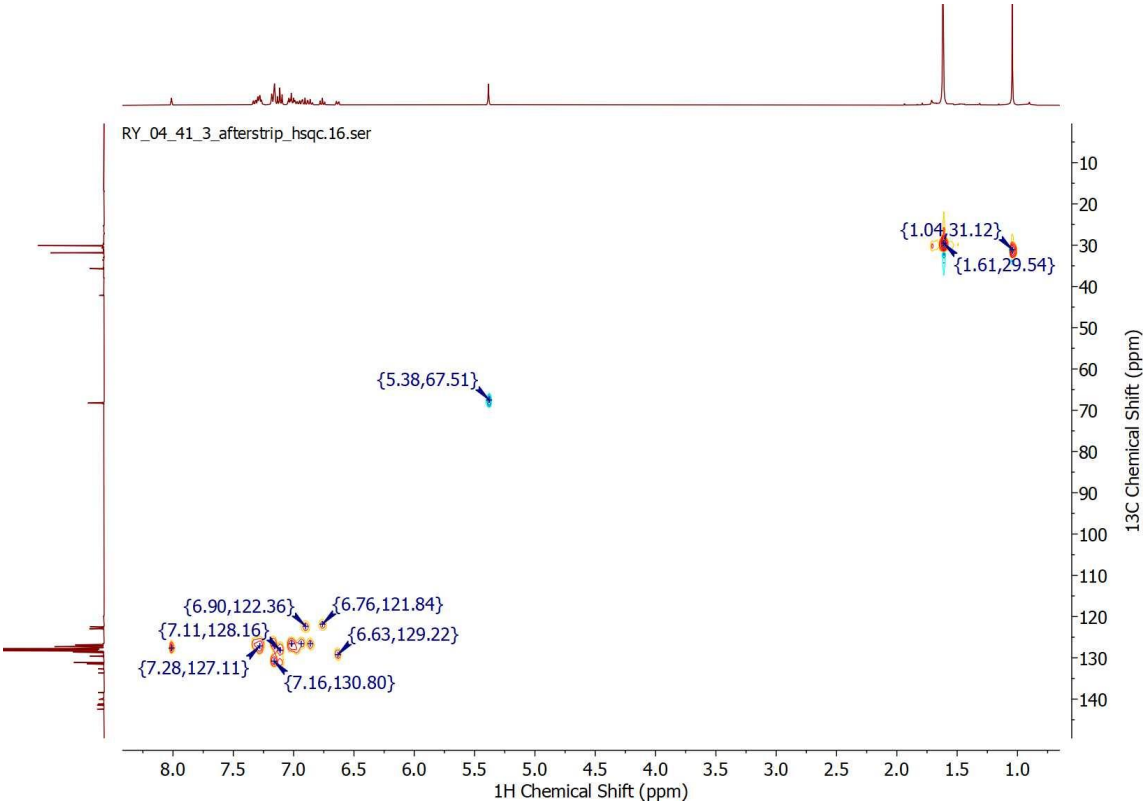


**Figure S47**. $^{1}H$-$^{13}C$ HSQC NMR spectrum of **4-Bn** ($C_6D_6$, 400 MHz, 25 °C).

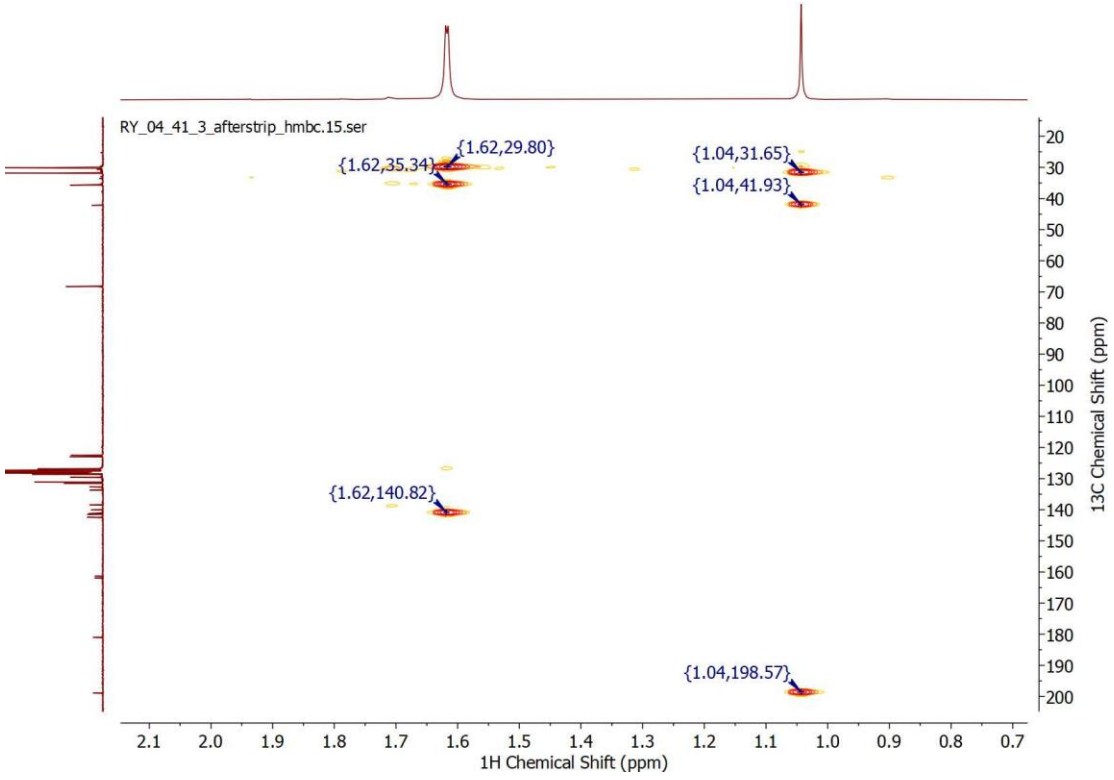


**Figure S48**. $^{1}H$-$^{13}C$ HMBC NMR spectrum-expansion of **4-Bn** ($C_6D_6$, 400 MHz, 25 °C).

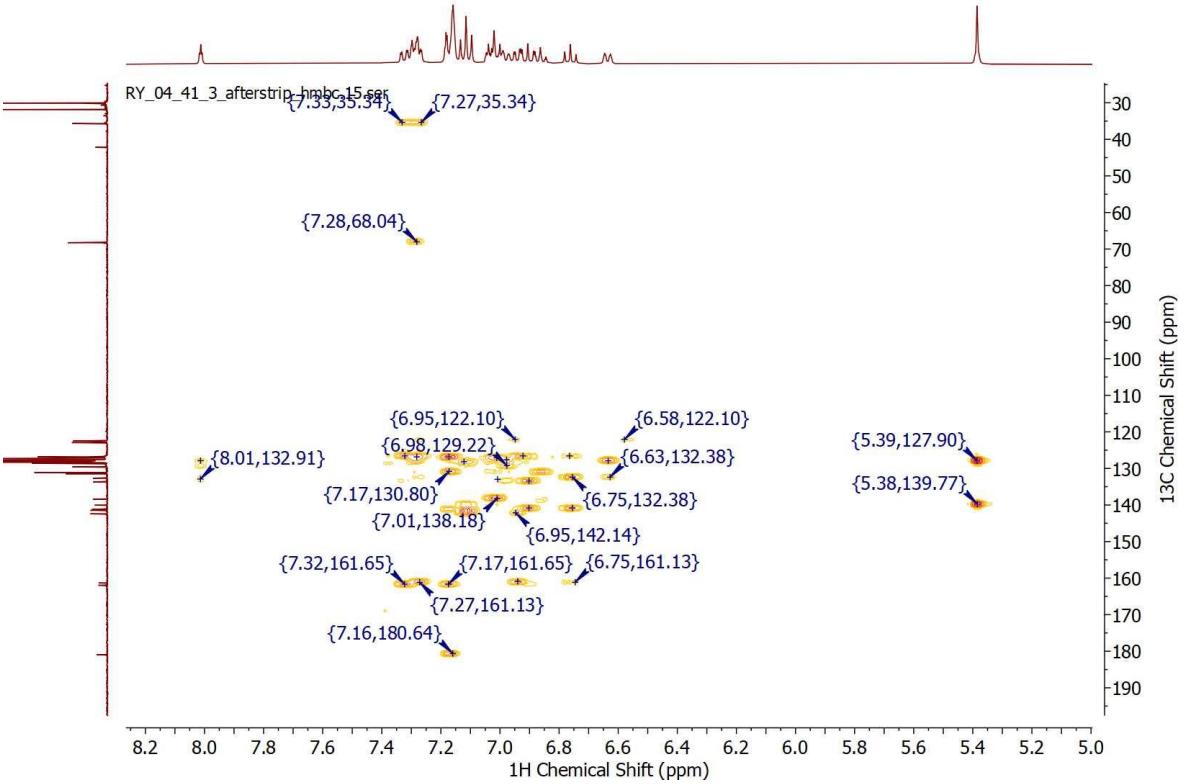


**Figure S49**. $^{1}H$-$^{13}C$ HMBC NMR spectrum-expansion of **4-Bn** ($C_6D_6$, 400 MHz, 25 °C).

## 4. X-ray crystallographic data

### 4.1. Procedure for data collection

X-Ray Intensity data were collected at 100 K on a Bruker Dual micro source D8 Venture diffractometer and PHOTON III detector running APEX3 software package of programs and using MoKα radiation (λ = 0.71073 Å).The data frames were integrated and multi-scan scaling was applied in APEX3. Intrinsic phasing structure solution provided all of the non-H atoms. The structure was refined using full-matrix least-squares refinement (SHELXL, Sheldrick G.M. 2015). The non-H atoms were refined with anisotropic displacement parameters and all of the H atoms were calculated in idealized positions and refined riding on their parent atoms. The refinement was carried out by minimizing the $wR_2$ function using $F^2$ rather than F values. $R_1$ is calculated to provide a reference to the conventional R value but its function is not minimized.

#### 4.1.1. Crystallographic data of 2

In the final cycle of refinement, 11557 reflections (of which 10619 are observed with $I > 2\sigma(I)$) were used to refine 406 parameters and the resulting $R_1$, $wR_2$ and S (goodness of fit) were 2.20%, 5.74% and 1.317, respectively.

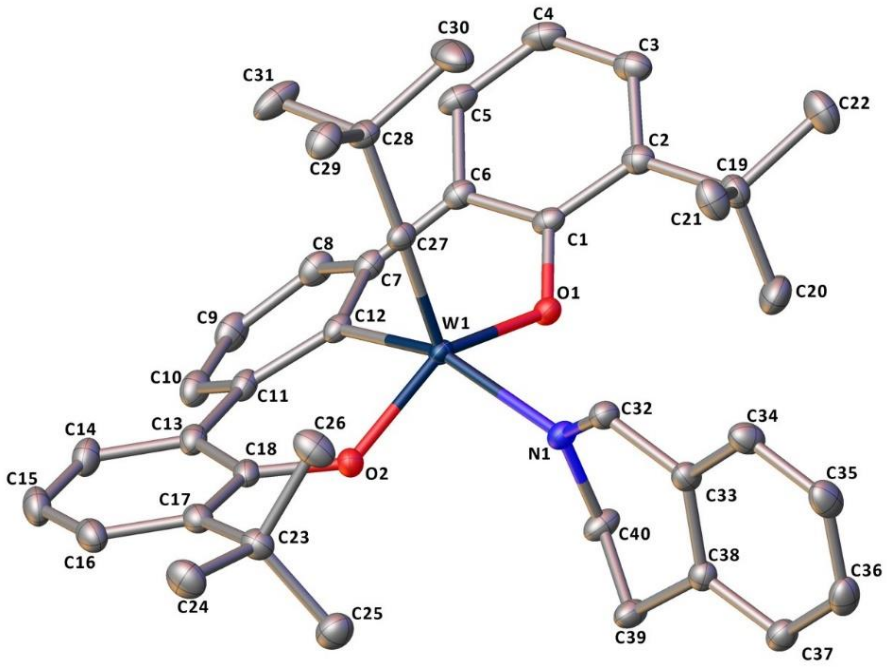


**Figure S50.** Solid-state molecular structure of **2**. Ellipsoids drawn at 50% probability. Hydrogen atoms are removed for clarity.

**Table S1**. Crystal data and structure refinement for **2**.

| | | |
|---|---|---|
| Identification code | rinku18 | |
| Empirical formula | $C_{40}H_{45}NO_2W$ | |
| Formula weight | 755.62 | |
| Temperature | 100(2) K | |
| Wavelength | 0.71073 Å | |
| Crystal system | Monoclinic | |
| Space group | $P2_1/n$ | |
| Unit cell dimensions | a = 13.2327(4) Å | a= 90°. |
| | b = 18.0672(5) Å | b= 97.2920(10)°. |
| | c = 14.0890(4) Å | g = 90°. |
| Volume | 3341.12(17) $Å^3$ | |
| Z | 4 | |
| Density (calculated) | 1.502 $Mg/m^3$ | |
| Absorption coefficient | 3.493 $mm^{-1}$ | |
| F(000) | 1528 | |
| Crystal size | 0.279 x 0.158 x 0.143 $mm^3$ | |
| Theta range for data collection | 1.918 to 32.836°. | |
| Index ranges | $-19\leq h\leq 19$, $-27\leq k\leq 26$, $-21\leq l\leq 21$ | |
| Reflections collected | 94414 | |
| Independent reflections | 11557 [R(int) = 0.0328] | |

| | |
|---|---|
| Completeness to theta = 25.242° | 99.9 % |
| Absorption correction | multi-scan |
| Refinement method | Full-matrix least-squares on $F^2$ |
| Data / restraints / parameters | 11557 / 0 / 406 |
| Goodness-of-fit on $F^2$ | 1.317 |
| Final R indices [I>2sigma(I)] | $R_1$ = 0.0220, $wR_2$ = 0.0574 [10619] |
| R indices (all data) | $R_1$ = 0.0250, $wR_2$ = 0.0585 |
| Extinction coefficient | n/a |
| Largest diff. peak and hole | 0.844 and -1.807 e.Å$^{-3}$ |

$R_1 = \Sigma(||F_o| - |F_c||) / \Sigma|F_o|$

$wR_2 = [\Sigma[w(F_o^2 - F_c^2)^2] / \Sigma[w(F_o^2)^2]]^{1/2}$

$S = [\Sigma[w(F_o^2 - F_c^2)^2] / (n-p)]^{1/2}$

$w = 1/[\sigma^2 (F_o^2)+(m*p)^2+n*p]$, $p = [\max(F_o^2,0)+ 2* F_c^2]/3$, m & n are constants.

### 4.1.2. Crystallographic data of 4-Me

The complex has two disordered regions in the methyl group C40 and the t-butyl group on C36. In the final cycle of refinement, 16702 reflections (of which 14213 are observed with $I > 2\sigma(I)$) were used to refine 385 parameters and the resulting $R_1$, $wR_2$ and S (goodness of fit) were 2.62%, 5.10 % and 1.028, respectively.

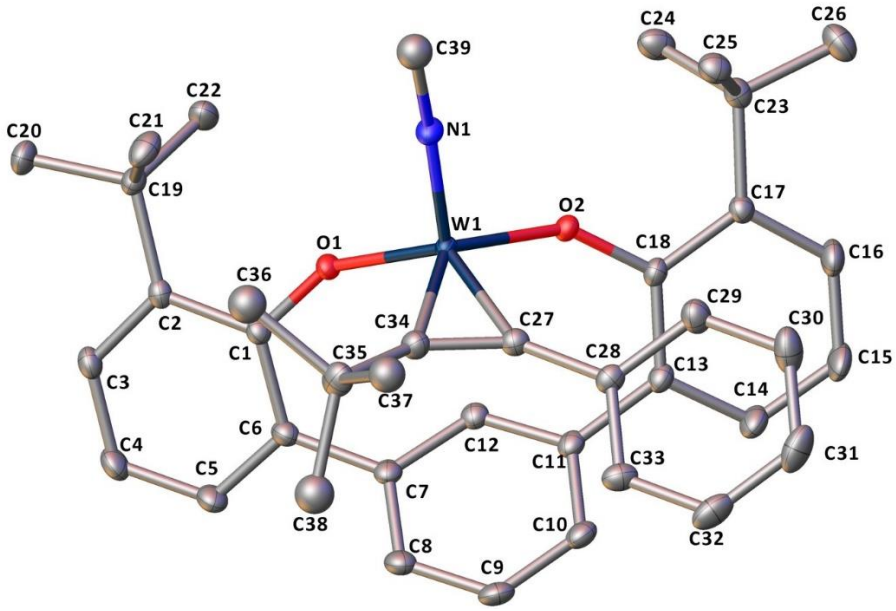


**Figure S51.** Solid-state molecular structure of **4-Me**. Ellipsoids drawn at 50% probability. Hydrogen atoms are removed for clarity.

**Table S2**. Crystal data and structure refinement for **4-Me**.

| | | |
|---|---|---|
| Identification code | rinku2 | |
| Empirical formula | $C_{39}H_{45}NO_2W$ | |
| Formula weight | 743.61 | |
| Temperature | 293(2) K | |
| Wavelength | 0.71073 Å | |
| Crystal system | Monoclinic | |
| Space group | C2/c | |
| Unit cell dimensions | a = 23.9026(19) Å | a= 90°. |
| | b = 11.1201(5) Å | b= 97.854(3)°. |
| | c = 26.2556(14) Å | g = 90°. |
| Volume | 6913.3(7) $Å^3$ | |
| Z | 8 | |
| Density (calculated) | 1.429 $Mg/m^3$ | |
| Absorption coefficient | 3.375 $mm^{-1}$ | |
| F(000) | 3008 | |
| Crystal size | 0.152 x 0.114 x 0.024 $mm^3$ | |
| Theta range for data collection | 2.023 to 36.334° | |
| Index ranges | $-39\leq h\leq 39$, $-18\leq k\leq 18$, $-43\leq l\leq 43$ | |
| Reflections collected | 157067 | |
| Independent reflections | 16702 [R(int) = 0.0635] | |
| Completeness to theta = 25.242° | 99.4 % | |
| Absorption correction | Semi-empirical from equivalents | |
| Max. and min. transmission | 0.9278 and 0.7247 | |
| Refinement method | Full-matrix least-squares on $F^2$ | |
| Data / restraints / parameters | 16702 / 0 / 385 | |
| Goodness-of-fit on $F^2$ | 1.028 | |
| Final R indices [I>2sigma(I)] | $R_1$ = 0.0262, $wR_2$ = 0.0510 [14213] | |
| R indices (all data) | $R_1$ = 0.0342, $wR_2$ = 0.0545 | |
| Extinction coefficient | n/a | |
| Largest diff. peak and hole | 1.361 and -1.348 $e.Å^{-3}$ | |

$R_1 = \Sigma(||F_o| - |F_c||) / \Sigma|F_o|$

$wR_2 = [\Sigma[w(F_o^2 - F_c^2)^2] / \Sigma[w(F_o^2)^2]]^{1/2}$

$S = [\Sigma[w(F_o^2 - F_c^2)^2] / (n-p)]^{1/2}$

$w = 1/[\sigma^2 (F_o^2)+(m*p)^2+n*p]$, $p = [\max(F_o^2,0)+ 2* F_c^2]/3$, m & n are constants.

### 4.1.3. Crystallographic data of 4-Ph

In the final cycle of refinement, 9050 reflections (of which 8223 are observed with $I > 2\sigma(I)$) were used to refine 442 parameters and the resulting $R_1$, $wR_2$ and S (goodness of fit) were 2.08%, 4.52% and 1.035, respectively.

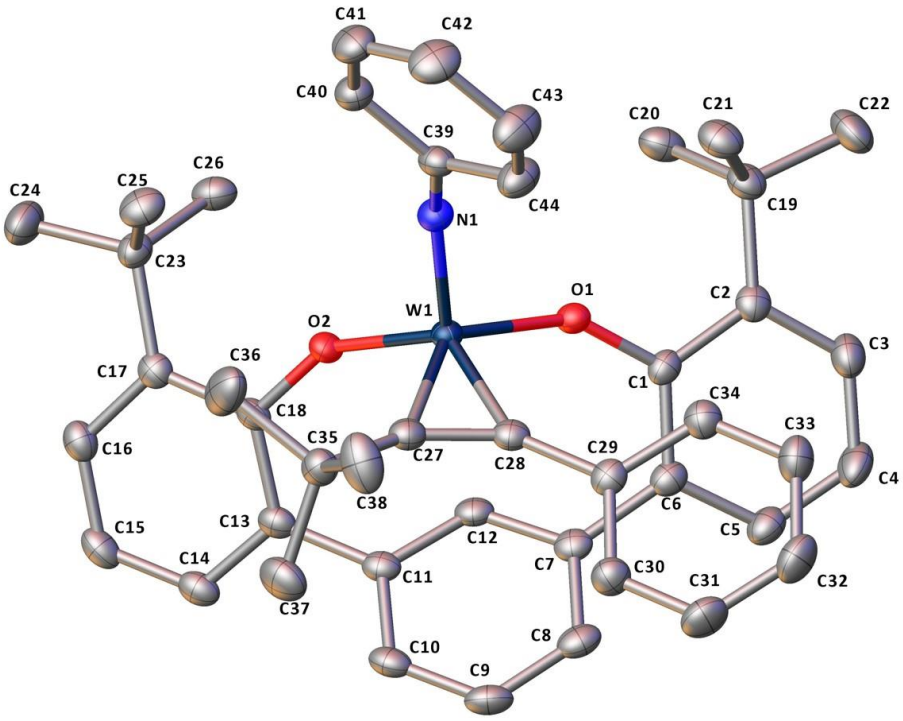


**Figure S52.** Solid-state molecular structure of **4-Ph**. Ellipsoids drawn at 50% probability. Hydrogen atoms are removed for clarity.

**Table S3**. Crystal data and structure refinement for **4-Ph**.

| | | |
|---|---|---|
| Identification code | rinku33 | |
| Empirical formula | $C_{44}H_{47}NO_2W$ | |
| Formula weight | 805.67 | |
| Temperature | 100(2) K | |
| Wavelength | 0.71073 Å | |
| Crystal system | Triclinic | |
| Space group | P-1 | |
| Unit cell dimensions | a = 9.3557(5) Å | a= 101.459(10)°. |
| | b = 11.8178(5) Å | b= 91.875(10)°. |
| | c = 16.8483(9) Å | g = 99.739(2)°. |
| Volume | 1795.12(16) $Å^3$ | |
| Z | 2 | |
| Density (calculated) | 1.491 $Mg/m^3$ | |
| Absorption coefficient | 3.255 $mm^{-1}$ | |

| | |
|---|---|
| F(000) | 816 |
| Crystal size | 0.650 x 0.084 x 0.075 $mm^3$ |
| Theta range for data collection | 1.951 to 28.538° |
| Index ranges | $-12 \leq h \leq 12$, $-15 \leq k \leq 15$, $-22 \leq l \leq 22$ |
| Reflections collected | 96677 |
| Independent reflections | 16702 [R(int) = 0.0635] |
| Completeness to theta = 25.242° | 99.9 % |
| Absorption correction | Semi-empirical from equivalents |
| Max. and min. transmission | 0.9278 and 0.7247 |
| Refinement method | Full-matrix least-squares on $F^2$ |
| Data / restraints / parameters | 16702 / 0 / 442 |
| Goodness-of-fit on $F^2$ | 1.035 |
| Final R indices [I>2sigma(I)] | $R_1 = 0.0208$, $wR_2 = 0.0434$ |
| R indices (all data) | $R_1 = 0.0258$, $wR_2 = 0.0452$ |
| Extinction coefficient | n/a |
| Largest diff. peak and hole | 0.875 and -0.477 e.$Å^{-3}$ |

$R_1 = \Sigma(||F_o| - |F_c||) / \Sigma|F_o$

$wR_2 = [\Sigma[w(F_o^2 - F_c^2)^2] / \Sigma[w(F_o^2)^2]]^{1/2}$

$S = [\Sigma[w(F_o^2 - F_c^2)^2] / (n-p)]^{1/2}$

$w = 1/[\sigma^2 (F_o^2)+(m*p)^2+n*p]$, $p = [\max(F_o^2,0)+ 2* F_c^2]/3$, m & n are constants.

### 4.1.4. Crystallographic data of 4-Bn

The complex has five disordered regions in the Ph ring on C40, C41, C42, C43, and C44. It also has a high electron density peak at 0.76 Å from tungsten arising from anisotropic modelling of heavy metal atom. In the final cycle of refinement, 9366 reflections (of which 8548 are observed with $I > 2\sigma(I)$) were used to refine 436 parameters and the resulting $R_1$, $wR_2$ and S (goodness of fit) were 3.13%, 7.18% and 1.087, respectively.

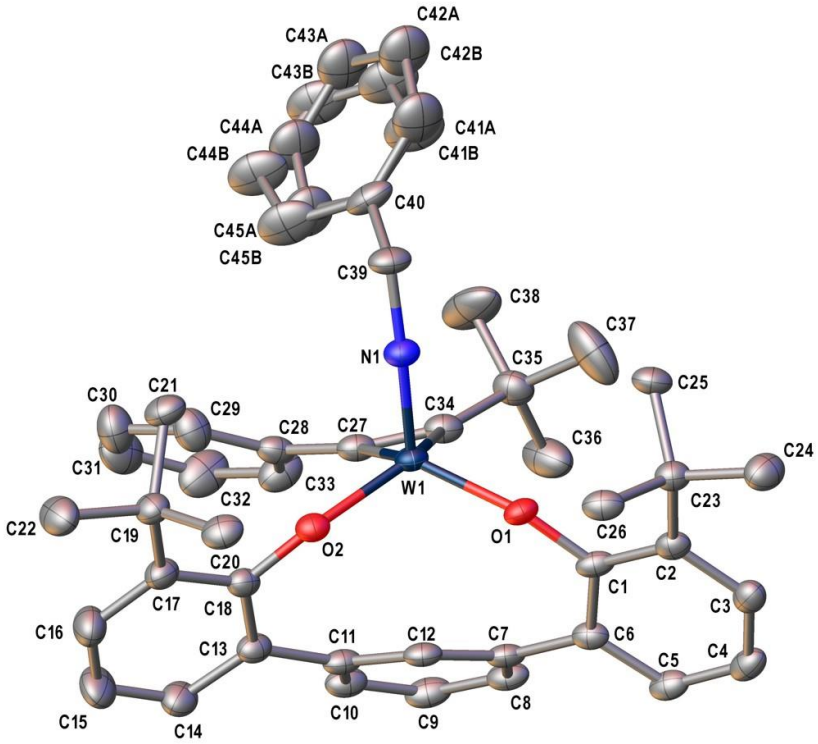


**Figure S53.** Solid-state molecular structure of **4-Bn**. Ellipsoids drawn at 50% probability. Hydrogen atoms are removed for clarity.

**Table S4**. Crystal data and structure refinement for **4-Bn**.

| | | |
|---|---|---|
| Identification code | rinku36 | |
| Empirical formula | $C_{45}H_{49}NO_2W$ | |
| Formula weight | 819.70 | |
| Temperature | 100(2) K | |
| Wavelength | 0.71073 Å | |
| Crystal system | Triclinic | |
| Space group | P-1 | |
| Unit cell dimensions | a = 9.425(2) Å | a= 95.897(5)°. |
| | b = 12.400(3) Å | b= 92.628(7)°. |
| | c = 16.608(3) Å | g = 106.096(6)°. |
| Volume | 1875.8(7) $Å^3$ | |
| Z | 2 | |
| Density (calculated) | 1.451 $Mg/m^3$ | |
| Absorption coefficient | 3.117 $mm^{-1}$ | |
| F(000) | 832 | |
| Crystal size | 0.650 x 0.084 x 0.075 $mm^3$ | |
| Theta range for data collection | 1.980 to 28.348° | |
| Index ranges | -12≤h≤12, -16≤k≤16, -22≤l≤22 | |
| Reflections collected | 90763 | |

| | |
|---|---|
| Independent reflections | 9366 [R(int) = 0.0553] |
| Completeness to theta = 25.242° | 99.9 % |
| Absorption correction | Semi-empirical from equivalents |
| Max. and min. transmission | n/a |
| Refinement method | Full-matrix least-squares on $F^2$ |
| Data / restraints / parameters | 9366 / 4 / 436 |
| Goodness-of-fit on $F^2$ | 1.087 |
| Final R indices [I>2sigma(I)] | $R_1$ = 0.0313, $wR_2$ = 0.0718 |
| R indices (all data) | $R_1$ = 0.0360, $wR_2$ = 0.0697 |
| Extinction coefficient | n/a |
| Largest diff. peak and hole | 4.021 and -1.546 e.Å$^{-3}$ |

$R_1 = \Sigma(||F_o| - |F_c||) / \Sigma|F_o$

$wR_2 = [\Sigma[w(F_o^2 - F_c^2)^2] / \Sigma[w(F_o^2)^2]]^{1/2}$

$S = [\Sigma[w(F_o^2 - F_c^2)^2] / (n-p)]^{1/2}$

$w= 1/[\sigma^2 (F_o^2)+(m*p)^2+n*p]$, $p = [\max(F_o^2,0)+ 2* F_c^2]/3$, m & n are constants.

## 5. References


1 S. Sarkar, K. P. McGowan, S. Kuppuswamy, I. Ghiviriga, K. A. Abboud and A. S. Veige, *J. Am. Chem. Soc.*, 2012, **134**, 4509–4512.

2 M. R. Monaco, P. Renzi, D. M. Scarpino Schietroma and M. Bella, *Org. Lett.*, 2011, **13**, 4546–4549.

3 M. A. Mercadante, C. B. Kelly, T. A. Hamlin, K. R. Delle Chiaie, M. D. Drago, K. K. Duffy, M. T. Dumas, D. C. Fager, B. L. C. Glod, K. E. Hansen, C. R. Hill, R. M. Leising, C. L. Lynes, A. E. Macinnis, M. R. McGohey, S. A. Murray, M. C. Piquette, S. L. Roy, R. M. Smith, K. R. Sullivan, B. H. Truong, K. M. Vailonis, V. Gorbatyuk, N. E. Leadbeater and L. J. Tilley, *Chem. Sci.*, 2014, **5**, 3983–3994.

4 X. Wang, G. Kehr, C. G. Daniliuc and G. Erker, *J. Am. Chem. Soc.*, 2014, **136**, 3293–3303.